INL/EXT-13-29961
Revision 1

Preliminary Scaling and Controls Analysis of an FHR-HTSE System

Idaho National Laboratory Summer 2013 Final Report

Rohit Upadhya
Shannon Bragg-Sitton
Piyush Sabharwall

January 2014

The INL is a U.S. Department of Energy National Laboratory
operated by Battelle Energy Alliance

Idaho National Laboratory

INL/EXT-13-29961
Revision 1

Preliminary Scaling and Controls Analysis of an FHR-HTSE System

Idaho National Laboratory Summer 2013 Final Report

Rohit Upadhya, Shannon Bragg-Sitton, and Piyush Sabharwall

January 2014

Idaho National Laboratory
Idaho Falls, Idaho 83415

http://www.inl.gov

Prepared for the
U.S. Department of Energy
Office of Nuclear Energy
Under DOE Idaho Operations Office
Contract DE-AC07-05ID14517

Preliminary Scaling and Controls Analysis of an FHR-HTSE System

Idaho National Laboratory Summer 2013 Final Report

INL/EXT-13-29961
Revision 1

January 2014

ABSTRACT

For new nuclear reactor system designs to be approved by regulatory agencies like the Nuclear Regulatory Commission (NRC), the details of system operation must be validated with respect to standards of safety, control, and output. A scaled experiment that replicates certain properties of the system can be used to validate compliance with regulatory standards, while avoiding the prohibitive cost and labor required to develop a fully functional prototype system; therefore, designing such an experiment is of special interest to current efforts to develop hybrid energy systems (HES) that integrate small modular reactors (SMRs), renewable energy systems, and industrial process applications such as hydrogen production and desalination. In addition, a scaled experiment can be an economical method of analyzing the interconnections between HES components and understanding the time constants associated between inter-component energy and information flows.

This report discusses the results of a preliminary scaling analysis done for the primary loop of a 300 $MWth$ Fluoride-Salt-Cooled High Temperature Reactor (FHR) that is coupled with a High-Temperature Steam Electrolysis system (HTSE), as well as the basic control logic that governs the primary components and the necessary hardware to achieve optimal functionality. The scaled facility will be a 1 $MWth$ system that uses Dowtherm A as the simulant fluid for Flibe (the coolant of choice for the primary loop of molten salt reactors), and can validate the heat transfer and steady-state operational requirements of the 300 $MWth$ prototype. The scaled facility matches the Prandtl and Reynolds numbers associated with steady-state operation of the FHR-HTSE's primary loop without having to deal with very high temperatures, flow rates, or power inputs. This will allow the facility to run experiments that analyze various thermophysical and fluid-dynamic properties that characterize reactor operation, such as pressure drops, radial temperature distribution, heat exchanger conditions. The facility also has potential to integrate additional components of the prototype system, such as intermediate thermal-hydraulics loops, real-time grid-demand data, energy storage, and HTSE.

CONTENTS

FIGURES

TABLES

ACRONYMS

CFD	Computational Fluid Dynamic
CIET	Compact Integral Effects Test
ESL	Energy Systems Laboratory
FHR	Fluoride-Salt-Cooled, High-Temperature Reactor
HES	Hybrid Energy System
HTSE	High-temperature steam electrolysis
IHX	Intermediate heat-exchanger
INL	Idaho National Laboratory
NHES	Nuclear Hybrid Energy System
NRC	Nuclear Regulatory Commission
VSD	Variable Speed Drive

Preliminary Scaling and Controls Analysis of an FHR-HTSE System

Idaho National Laboratory Summer 2013 Final Report

1. INTRODUCTION

The United States, and the world as a whole, is faced with unique and unprecedented challenges with regards to constructing an energy portfolio that can rapidly, effectively, and economically deal with issues of ecological collapse, energy security, and future demand for energy resources. These issues combine in such a way as to necessitate the development of zero-carbon energy systems that are both versatile and economic.

Hybrid energy systems (HES) offer a potential solution to all of the aforementioned challenges. HES can take many forms, but the most optimal design to meet current energy needs consists of an integration of base-load and intermittent energy sources, and in some designs, a further integration of industrial processes with energy production. Recent reports from Idaho National Laboratory (INL) have shown that hybrid energy systems, in scenarios with a high level of intermittent renewable penetration, provide better performance and economics than traditional systems.[1,2] Integration of renewables with nuclear systems in particular have been shown to be consistently better than traditional systems, as well as fossil-based HES. A value proposition from INL found that a system that integrates a Fluoride-Salt-Cooled High Temperature Reactor (FHR) with a High-Temperature Steam Electrolysis (HTSE) unit holds great promise for being an optimal nuclear hybrid energy system (NHES) design, in terms of economics and carbon emissions. [3] It is particularly important to note that an NHES design can allow a nuclear power plant to be both load-following and thermally efficient, as nuclear heat can be diverted to industrial processes during times of low demand (whereas with traditional nuclear systems, low demand leads to a shedding of thermal energy and a corresponding decrease in efficiency).

To further the development of FHR-HTSE systems (and NHES in general), it is necessary to take a closer look at the actual technical aspects of normal operation. This paper lays out a preliminary scaling analysis of a 300 $MWth$ FHR-HTSE's primary loop, so that various thermophysical and fluid-dynamic phenomena can be characterized and documented. Scaling is an effective method of duplicating process phenomena without actually building the system in question; in this particular case, a simple scaling analysis that matched the Prandtl and Reynolds numbers of the prototype system results in a 1 $MWth$ experiment that is non-nuclear (thus saving on the intense labor costs and safety regulations associated with nuclear experiments) and non-salt-based (saving on the safety regulations associated with toxic salts like Flibe). However, the applicability of this analysis' results to an actual, full-scale FHR-HTSE are limited because there does not yet exist an actual, rigorous design for a prototype FHR-HTSE. Hence, some of the parameters (specifically, the geometry) chosen to represent the values of the prototype will most likely change in the future.

In addition to the scaling analysis, a rudimentary open-loop controls algorithm was developed to relate various subsystems to one another, in terms of thermal and electrical energy flows. This algorithm

1. Garcia, Humberto E., Mohanty, Amit, Lin, Wen-Chiao, Cherry, Robert S., "Dynamic analysis of hybrid energy systems under flexible operation and variable renewable generation – Part I: Dynamic performance analysis," *Energy*, 2013.
2. Garcia, Humberto E., Mohanty, Amit, Lin, Wen-Chiao, Cherry, Robert S., "Dynamic analysis of hybrid energy systems under flexible operation and variable renewable generation – Part II: Dynamic cost analysis," *Energy*, 2013.
3. Bragg-Sitton, S. M., Boardman, R., McKellar, M., Garcia, H., Wood, R., Sabharwall, P., and Rabiti, C., "Value Proposition for Load-Following Small Modular Reactor Hybrid Energy Systems," Idaho National Laboratory, INL/EXT-13-29298, May 2013.

can serve as the basis for a closed-loop feedback controls system that will be necessary to develop in the near future.

The proposed experiment should be seen not as a complete system, but the first iteration in a series of iterations that can continuously add on additional components that simulate the full-scale prototype. The add-ons can take the form of both hardware and software. For instance, the load-shifting qualities of the system can be tested using simulated grid-demand data, so that the load-following dynamics can be validated, along with its result fluid dynamics. In addition, the current method of simulating the intermediate heat-exchangers (IHX) with a fan can be replaced with scaled loops, and even attached to hardware that simulates the dynamics of HTSE and power loops.

2. PRIMARY LOOP SCALING ANALYSIS

Scaling analysis is a technique that seeks to scale down a large, complex system (the prototype) so the primary phenomena of interest can be characterized and studied in a smaller, simpler facility (the model), resulting in less costs and labor.[4] It is an important method in the research and development of nuclear energy, and has been used in many laboratories for thermal-hydraulics analysis, code validation, and Nuclear Regulatory Commission (NRC) licensing purposes.[5]

The analysis done here is very preliminary, as it only seeks to replicate properties of normal operation, and does not include scenarios such as transient or accident events.

2.1 Analysis of Fluids

Flibe is the chosen molten salt that is used in the primary loop for all standard FHRs. It was chosen due to its high heat capacity, high boiling point, and negative feedback coefficient (meaning that in the case of an accident, and the resulting higher temperatures in the core, the reactor will begin to shut itself down). However, Flibe poses difficulties for experimentation due to its toxic nature and high operating temperatures in the prototype system (up to 850℃). Thus, it is desirable to find a simulant fluid that mimics the important characteristics of Filbe at lower temperatures.

The Prandtl number is an important dimensionless number that characterizes the heat transfer properties of a fluid. Thus, it is important to preserve this number in a scaled experiment with respect to the prototype that the experiment is modeling.

An investigation into possible simulant fluids that preserve the Prandtl number of Flibe at various temperatures was conducted by Bardet and Peterson,[6] and proposed Dowtherm A as a possible fit. Subsequent analysis at UC Berkeley for their Compact Integral Effects Test (CIET) found that Dowtherm A, at temperatures ranging from 57 – 117℃, matched the Prandtl number of Flibe at temperatures ranging from 600 – 800℃.

However, the scaled experimental facility at INL will simulate an FHR with a core temperature range of 800 – 850℃. Thus, an analysis was conducted to see whether Dowtherm A would match the Prandtl number of Flibe across this temperature range.

4. Zuber, Novak, "Scaling: From Quanta to Nuclear Reactors," Nuclear Engineering and Design, Vol. 240, No. 8, 2010, P1986-1996.
5. Reyes, Jose N. Jr., Lawrence Hochreiter, "Scaling analysis for the OSU AP600 Test Facility (APEX)," *Nuclear Engineering and Design*, Vol. 186, No. 1–2, 1998, pp. 53–109.
6. Bardet, Philippe M., Per F. Peterson, "Options for Scaled Experiments for High Temperature Liquid Salt and Helium Fluid Mechanics and Heat Transfer," *Nuclear Technology*, Vol. 163, September 2008.

2.1.1 Thermophysical Properties of Flibe

Table 1 shows the equations of the thermophysical properties of Flibe, taken from a 2010 INL report on the properties of various liquid salts.[7] All temperature values are in Kelvin. The prototype 300 $MWth$ FHR reactor's primary loop has a temperature range of $800℃ - 850℃$. Table 2 shows the properties of Flibe across this temperature range. The graphs of the properties and trend-lines, to three significant figures, are shown in Figure 1.

7. Sohal, Manohar S., Matthias A. Ebner, Piyush Sabharwall, and Phil Sharpe, "Engineering Database of Liquid Salt Thermophysical and Thermochemical Properties," Idaho National Laboratory, INL/EXT-10-18297, March 2010.

Table 1. Temperature-dependent equations for the thermophysical properties of Flibe.

Property	Units	Equation	Source	Temperature Range
Density	$\frac{\text{kg}}{\text{m}^3}$	(1) $\rho = 2415.6 - 0.49072T$ (2) $\rho = 2763.7 - 0.687T$	(1) Zaghloul 2003 (2) Ignat'ev 2006[a]	(1) All temperatures (2) $T > 973K$
Dynamic Viscosity	$Pa - s$	$\mu = 0.000116e^{\frac{3755}{T}}$	Williams 2006	$873\ K < T < 1073\ K$
Kinematic Viscosity	$\frac{m^2}{s}$	$\nu = \frac{\mu}{\rho} = \frac{0.000116e^{\frac{3755}{T}}}{2763.7 - 0.687T}$	Analytically derived	$(T > 973K)$ and/or $(873\ K < T < 1073\ K)$
Specific Heat	$\frac{J}{kg - K}$	2415.78	Williams 2006	$973\ K$
Thermal Conductivity	$\frac{W}{m - K}$	1	Williams 2001	All temperatures
Prandtl	$dimensionless$	$Pr = 0.28023e^{\frac{3755}{T}}$	Analytically derived	?

a. Used in all following calculations involving density.

Table 2. Thermophysical properties of Flibe from 800 to 850°C.

T[C]	Vis [Pa-s]	Spec Heat [J/kg-K]	Th. Cond [W/m-K]	Density [kg/m^3]	Kin Vis [m^2/s]	Prandtl
800	0.003837725	2415.78	1	2026.44595	1.89382E-06	**9.27**
805	0.003775953	2415.78	1	2023.01095	1.8665E-06	**9.12**
810	0.003715731	2415.78	1	2019.57595	1.83986E-06	**8.98**
815	0.00365701	2415.78	1	2016.14095	1.81387E-06	**8.83**
820	0.003599742	2415.78	1	2012.70595	1.78851E-06	**8.7**
825	0.00354388	2415.78	1	2009.27095	1.76376E-06	**8.56**
830	0.003489379	2415.78	1	2005.83595	1.73961E-06	**8.43**
835	0.003436197	2415.78	1	2002.40095	1.71604E-06	**8.3**
840	0.003384293	2415.78	1	1998.96595	1.69302E-06	**8.18**
845	0.003333626	2415.78	1	1995.53095	1.67055E-06	**8.05**
850	0.003284159	2415.78	1	1992.09595	1.64859E-06	**7.93**

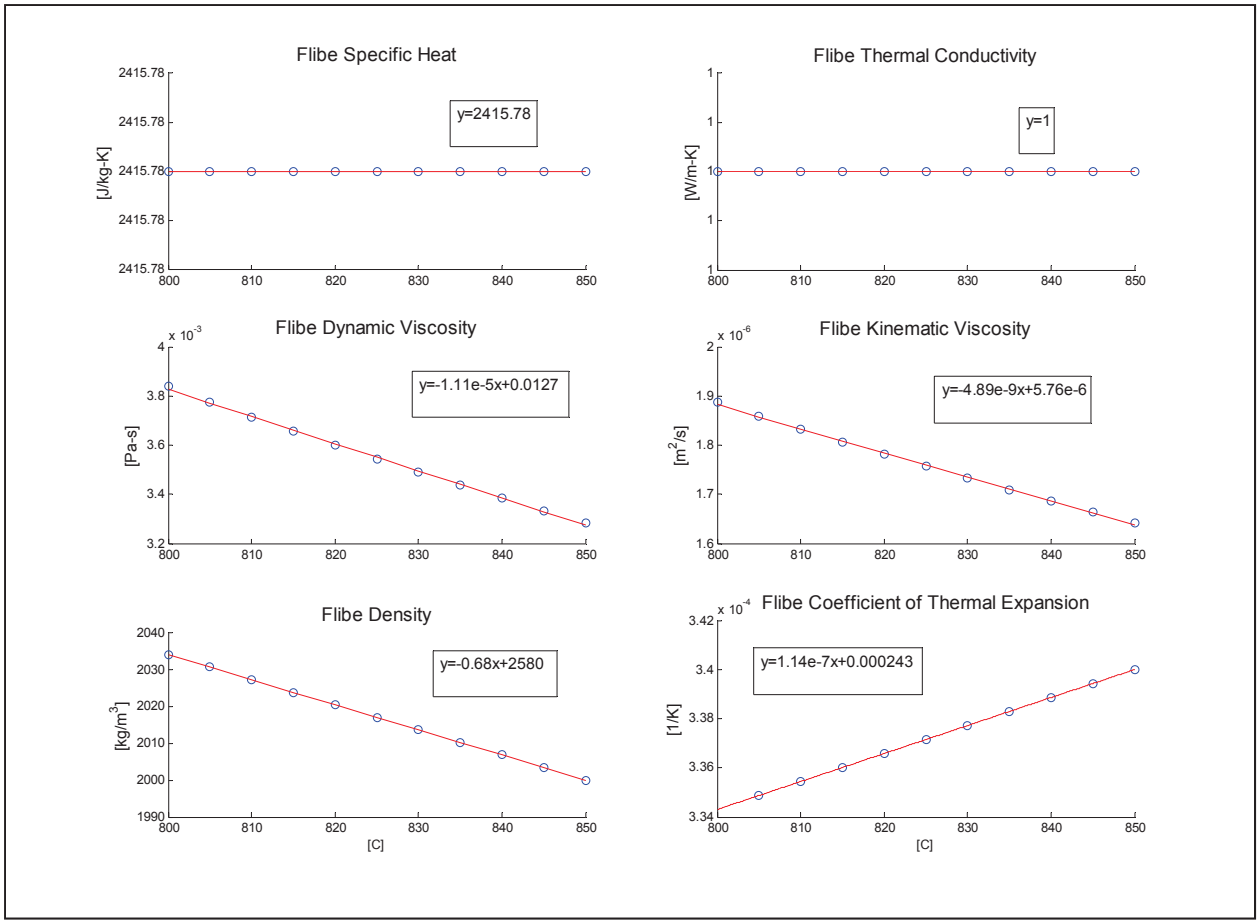

Figure 1. Graphs of the thermophysical properties of Flibe as a function of temperature.

It is necessary to find the average values of density and dynamic viscosity over the core's temperature range. The standard average value of a function equation is used[8]:

$$\frac{1}{b-a}\int_a^b f(x)dx = \frac{1}{T_b - T_a}\int_{T_a}^{T_b} f(T)dT = \frac{1}{50}\int_{1073.15\ K}^{1123.15\ K} f(T)dT$$

Thus the average values of the aforementioned properties are as follows:

$$\bar{\mu} = \frac{1}{50}\int_{1073.15\ K}^{1123.15\ K} (0.000116e^{\frac{3755}{T}})dT = 3.5496 * 10^{-3}\ Pa - s$$

$$\bar{\rho} = \frac{1}{50}\int_{1073.15\ K}^{1123.15\ K} (2763.7 - 0.687T)dT = 2009.27\frac{kg}{m^3}$$

These values can be used to also find the average value of the kinematic viscosity.

$$\frac{\bar{\mu}}{\bar{\rho}} = \bar{\nu} = \frac{3.5496 * 10^{-3}\ Pa - s}{2009.27\frac{kg}{m^3}} = 1.7666 * 10^{-6}\frac{m^2}{s}$$

8. Stewart, James, *Multivariable Calculus: Early Transcendentals*, 6th Edition, Cengage Learning, 2007.

2.1.2 Thermophysical Properties of Dowtherm A

Dowtherm A is a heat transfer fluid manufactured by various companies. As pointed out by Bardet and Peterson 2008, Dowtherm's properties makes it ideal for use as a simulant fluid for replicating thermophysical properties of Flibe.

Table 3 shows data taken from Dow Chemical's technical sheet for Dowtherm A.[9] The Prandtl number was calculated analytically. The green section of Table 3 signifies the range over which the Prandtl number for Dowtherm matches the Prandtl number of Flibe over the prototype reactor's temperature range. The graphs of the properties over this range are shown in Figure 2, along with linear-fit trend-lines.

Table 3. Thermophysical properties of Dowtherm A from 115 to 215°C.

T[C]	Vis [Pa-s]	Spec Heat [J/kg-K]	Th. Cond [W/m-K]	Density [kg/m^3]	Prandtl
115	0.00082	1842	0.1235	982.3	**12.23**
120	0.00077	1856	0.1227	978.1	**11.65**
125	0.00073	1870	0.1219	973.8	**11.2**
130	0.0007	1884	0.1211	969.5	**10.89**
135	0.00067	1898	0.1203	965.2	**10.57**
140	0.00064	1912	0.1195	960.9	**10.24**
145	0.00061	1926	0.1187	956.6	**9.9**
150	0.00058	1940	0.1179	952.2	**9.54**
155	0.00056	1954	0.1171	947.8	**9.34**
160	0.00053	1968	0.1163	943.4	**8.97**
165	0.00051	1982	0.1155	938.9	**8.75**
170	0.00049	1996	0.1147	934.5	**8.53**
175	0.00047	2010	0.1139	930	**8.29**
180	0.00046	2023	0.1131	925.5	**8.23**
185	0.00044	2037	0.1123	920.9	**7.98**
190	0.00042	2051	0.1115	916.4	**7.73**
195	0.00041	2065	0.1107	911.8	**7.65**
200	0.00039	2079	0.1099	907.1	**7.38**
205	0.00038	2093	0.1091	902.5	**7.29**
210	0.00037	2107	0.1083	897.8	**7.2**
215	0.00035	2120	0.1075	893.1	**6.9**

9. The Dow Chemical Company, "Dowtherm A Heat Transfer Fluid Product Technical Data," 1997.

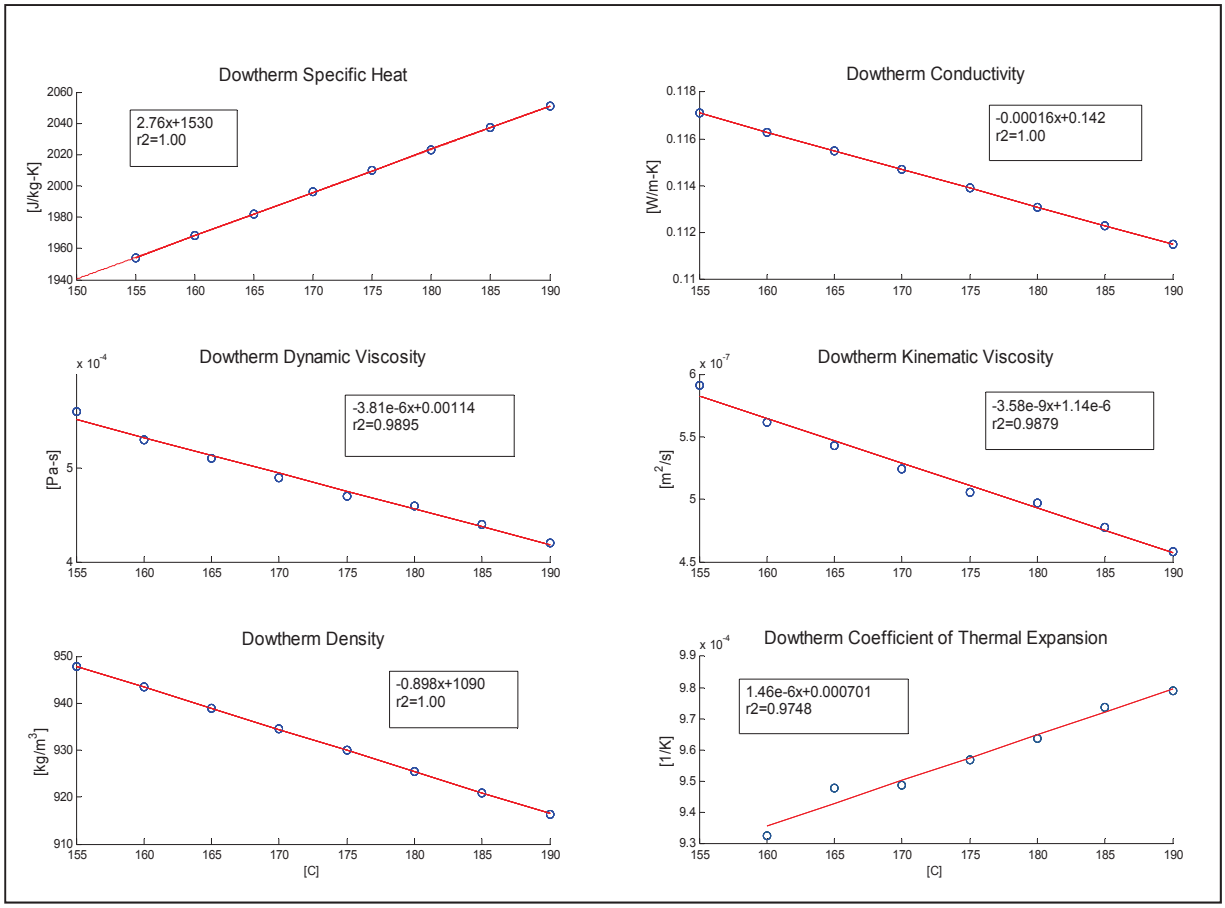

Figure 2. Thermophysical properties of Dowtherm A as a function of temperature.

The linear fits for dynamic viscosity, kinematic viscosity, and the coefficient of thermal expansion had low values of r^2. Thus, Excel was used to find better fits. The following equations were found:

$$\mu = 0.5044T^{-1.35}$$

$$\nu = -2.579 * 10^{-12}T^3 + 1.362 * 10^{-9}T^2 - 2.426 * 10^{-7}T + 1.508 * 10^{-5}$$

$$\beta = -3.716 * 10^{-10}T^4 + 2.614 * 10^{-7}T^3 - 6.884 * 10^{-5}T^2 + 8.049 * 10^{-3}T - 0.3517$$

2.1.3 Matching the Prandtl Number

The data from the Dowtherm table was graphed in MATLAB, and used to calculate a cubic trend-line for the Prandtl number. This is shown in Figure 3. Solving for the Prandtl numbers of 9.27 and 7.93, the specific temperature range of Dowtherm A that replicates Flibe's Prandtl number on [800℃, 850℃] is [155.865℃, 186.217℃]. Rounding to three significant figures, Dowtherm's appropriate temperature range is [156℃, 186℃]. Figure 4 shows the matching of Flibe and Dowtherm's Prandtl numbers over their respective temperature ranges.

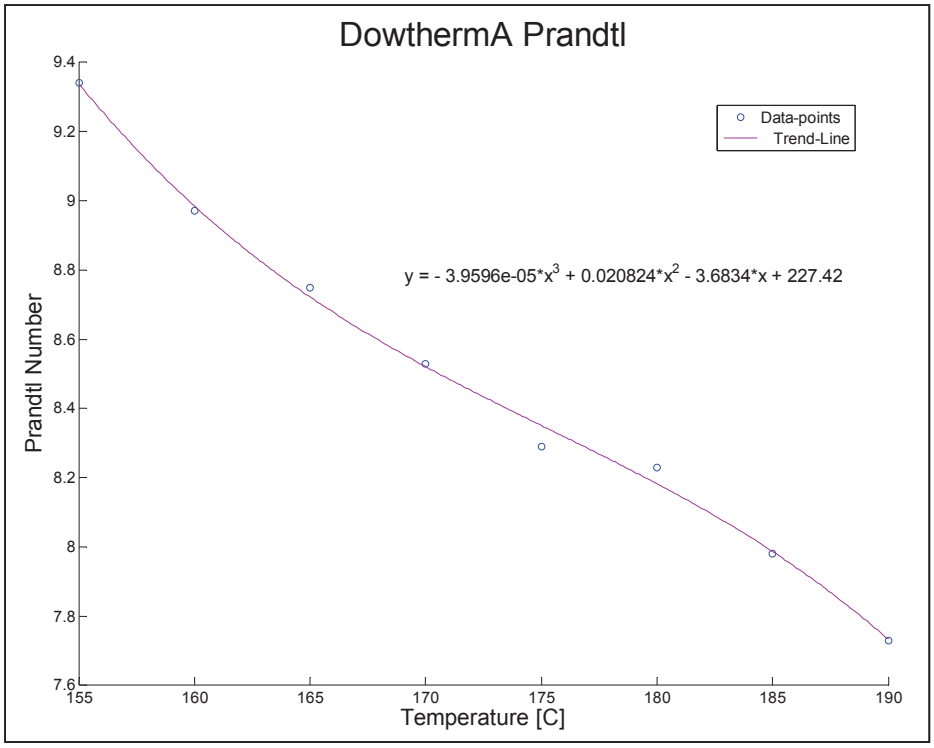

Figure 3. Graph of Dowtherm A's Prandtl number from 155 to 190°C.

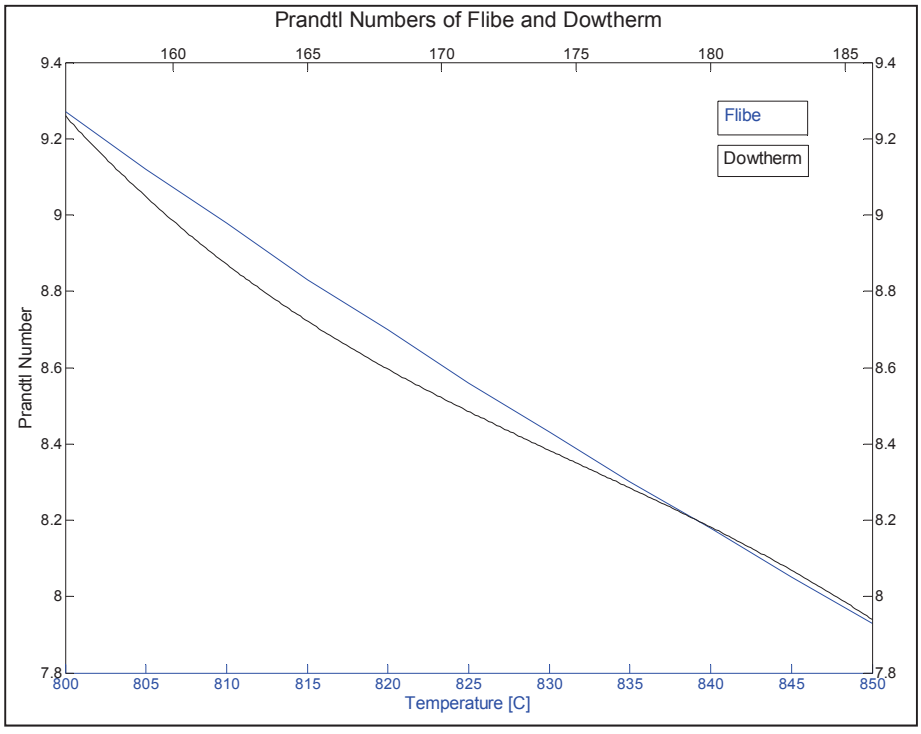

Figure 4. Graph of Flibe and Dowtherm's Prandtl numbers over their respective temperature ranges.

Now we can find different properties' average values for Dowtherm across the scaled temperature range, using the fitted equations as the $f(x)$ for the average value integral.

$$\bar{\rho} = \frac{1}{186-156}\int_{156}^{186}(-0.0898T + 1090)dT = 936.442\,\frac{kg}{m^3}$$

$$\bar{\nu} = \frac{1}{186-156}\int_{156}^{186}(-2.579 * 10^{-12}T^3 + 1.362 * 10^{-9}T^{-9} - 2.426 * 10^{-7}T + 1.508 * 10^{-5})dT$$
$$= 5.2379 * 10^{-7}\,\frac{m^2}{s}$$

2.2 Analysis of Geometry and Subcomponents

Settling on the fluids gives us some parameters for the scaled facility, but it is still necessary to analyze additional sections of the prototype system to settle on the geometry. However, there are some unique challenges here—specifically, the fact that there is no actual, concrete design for a 300 MW_{th} FHR-HTSE. The best this analysis can do is estimate what the approximate geometry might be, and use that to derive some rough numbers as to what a rigorously scaled facility might look like. The resulting facility, in turn, can provide data on what a full-scale design should look like, and which parameter values work and do not work.

2.2.1 Scaling the Power and Mass Flow Rate

A relation between the thermal power and primary leg mass flow rate of the scaled experiment can be derived from the thermophysical properties of Flibe and Dowtherm, and known design parameters of the 300 $MWth$ FHR. Using the steady-flow thermal energy equation:

$$q_m = \dot{m}_m c_{p,m} \Delta T_m$$

Table 4 lists the definitions and known values for the variables (as well as the variables for the steady-flow thermal energy equation of the prototype reactor).

Table 4. Variables and values relevant to the steady-state thermal energy equation across the core.

Symbol	Definition	Value
ΔT_m	Temperature difference across the core of the scaled model	30 K (156℃ − 186℃)
ΔT_p	Temperature difference across the core of the prototype reactor	50 K (800℃ − 850℃)
q_m	Heat input of the scaled model	TBD
q_p	Thermal power of the prototype reactor	$300MW$
$\dot{m}_m$	Mass flow rate of primary leg the scaled model	TBD
$\dot{m}_p$	Mass flow rate of the primary leg of the prototype reactor	$2485\,\frac{kg}{s}$
$c_{p,m}$	Specific heat of Dowtherm over the temperature range of the scaled model's primary loop	$1998.5\,\frac{J}{kg-K}$
$c_{p,p}$	Specific heat of Flibe over the temperature range of the prototype reactor	$2415.78\,\frac{J}{kg-K}$

Inserting the known quantities:

$$q_m = \dot{m}_m(1998.5)(30) = 59955\dot{m}_m$$

Thus, we have a linear relationship between the power and mass flow-rate of the model.

We also derive an equation that relates heat input, pipe diameter, and flow velocity, starting from the definition of mass flow rate:

$$\dot{m}_m = \overline{\rho_m} A_m u_m = \rho_m \left(\frac{\pi D_m^2}{4}\right) u_m$$

Table 5 lists the definitions and values for these new variables.

Table 5. Variables and values for the modified steady-state thermal energy equation.

Symbol	Definition	Value
$\overline{\rho_m}$	Average density of Dowtherm over the core temperature range	$936.442\,\frac{kg}{m^3}$
A_m	Cross-sectional area of the model's primary leg	TBD
u_m	Flow velocity of Dowtherm through the primary leg	TBD
D_m	Diameter of the model's primary leg	TBD

Plugging in the above equation into the model heat to model mass flow rate equation and re-arranging the equation to get the known values on one side, the following relation emerges:

$$\frac{q_m}{\rho_m \left(\frac{\pi D_m^2}{4}\right) u_m} = 59955 \rightarrow \frac{q_m}{D_m^2 u_m} = \frac{59955(936.442)\pi}{4} = 44095693.023$$

$$q_m = 44095693.023 D_m^2 u_m$$

2.2.2 Matching the Reynolds Number

If we assume that the thermal power of the model is going to be the variable, then the above equation has two unknowns to solve for. We can derive a second equation to solve for these unknowns by scaling the Reynolds number.

Scaling the Reynolds number is advisable as this allows the model to duplicate the prototype's fluid dynamics--specifically, the flow regime and the friction factor. However, there are trade-offs in focusing on the Reynolds number, which warrants the latter section on discussing possible alternative criteria.

When the Reynolds number between the model and the prototype is preserved, a relation between the fluid velocity and the pipe diameter emerges.

$$(Re)_R = \left(\frac{uD}{\nu}\right)_R = 1 \rightarrow \frac{u_m D_m}{\overline{\nu_m}} = \frac{u_p D_p}{\overline{\nu_p}}$$

The definitions and values of the variables are listed in Table 6.

Table 6. Variables and values for the Reynolds number scaling relation.

Symbol	Definition	Value
u_m	Mean flow velocity of Dowtherm across the primary leg	TBD
u_p	Mean flow velocity of Flibe across the primary leg	TBD
D_m	Diameter of the model's primary leg	TBD
D_p	Diameter of the prototype's primary leg pipe	TBD
$\overline{\nu_m}$	Average kinematic viscosity of Dowtherm across the primary leg's temperature difference	$5.2379 * 10^{-7} \frac{m^2}{s}$
$\overline{\nu_p}$	Average kinematic viscosity of Flibe across the prototype core's temperature difference	$1.7666 * 10^{-6} \frac{m^2}{s}$

Re-arranging the known values to one side, the following ratio emerges:

$$\frac{u_m D_m}{u_p D_p} = \frac{\overline{\nu_m}}{\overline{\nu_p}} = 0.2965$$

$$u_m D_m = 0.2965 u_p D_p$$

2.2.3 Pipe Diameter and Flow Velocity

Finding standard numbers for the pipe diameter and average flow velocity of the prototype $300MWth$ reactor is tricky, as there is no actual design that has this thermal power; thus, it is necessary to estimate these numbers based on other reactor designs.

If we can settle on the flow-velocity, the diameter and cross-sectional area can be derived. Using the mass flow rate equation:

$$\dot{m}_p = \overline{\rho_p} A_p u_p \rightarrow A_p = \frac{\dot{m}_p}{\overline{\rho_p} u_p} = \frac{2485}{(2009.27) u_p} = \frac{1.237}{u_p}$$

Thus the diameter can also be derived:

$$A_p = \frac{\pi D_p^2}{4} \rightarrow D_p = \sqrt{\frac{4(\frac{1.237}{u_p})}{\pi}} = \sqrt{\frac{1.575}{u_p}}$$

Thus, we can see the range of different diameter values of the 300 $MWth$ prototype as a function of the different possible flow velocities. Table 7 documents these values.

Table 7. Values of prototype diameter and velocity-diameter product as a function of velocity.

u_p	D_p	$u_p D_p$
0.5	1.775	0.887
1	1.255	1.255
1.5	1.025	1.537
2	0.887	1.775
2.5	0.794	1.984
3	0.725	2.174

Now we further develop the two independent relations we derived earlier:

$$q_m = 44095693.023 D_m^2 u_m$$
$$u_m D_m = 0.2965 u_p D_p$$

We can plug the second equation into the first:

$$q_m = 44095693.023 D_m \left(0.297 u_p D_p\right) = 13074421.928 D_m (u_p D_p)$$

Solving for D_m:

$$D_m = \frac{q_m}{13074421.928\left(u_p D_p\right)}$$

$$u_m = \frac{0.2965 u_p D_p}{D_m} = \frac{0.2965 u_p D_p}{\frac{q_m}{13074421.928\left(u_p D_p\right)}} = \frac{3876580.614\left(u_p D_p\right)^2}{q_m}$$

Thus, for various values of u_p, we can plot the model's diameter and velocity as a function of power. Figure 5 shows the results of the relations from 500 kW to 1500 kW.

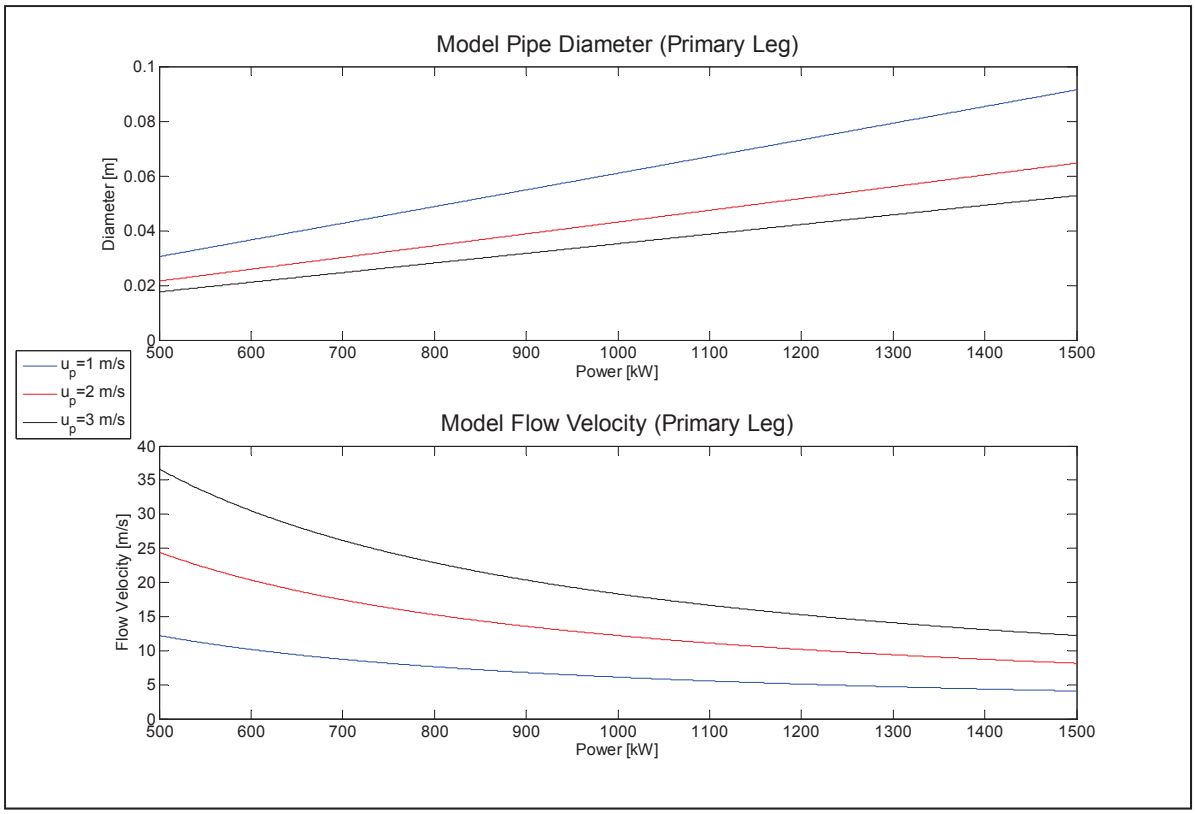

Figure 5. Graph of the model's diameter and flow velocity as a function of power, for three values of prototype flow velocity.

To settle on a flow velocity of the prototype reactor, a brief survey of the design parameters used for general molten salt reactors was done, the results of which are shown in Table 8.

Table 8. Surveyed designs of small FHRs, their thermal power, and their primary leg flow velocity.

Design	Thermal Power [MWth]	Flow Velocity [m/s]	Reference
smAHTR	125	1.1	Greene et al. 2012[10]
MOSART	2400	0.5	Jianjun et al. 2013[11]
MSBR	2250	1.47	Cammi et al. 2011[12]
MOSART	2400	0.5	Xiao et al. 2012[13]
AHTR	3400	2.09	Avigni and Petrovic 2013[14]

There appears to be no real correlation between thermal power and primary loop flow velocity. Thus, a rough average leads us to settle on a primary leg flow velocity of $1\frac{m}{s}$, which is also close to the smAHTR's flow velocity, the design that is closest to our $300\ MWth$ prototype.

Thus, the equations for model diameter and velocity become:

$$D_m = \frac{q_m}{13074421.928(1.255)} = \frac{q_m}{16406699.84}$$
$$u_m = \frac{3876580.614(1.255)^2}{q_m} = \frac{6104456.248}{q_m}$$

If we assume that the power is $1\ MW$, then the diameter and velocity are known:

$$D_m = \frac{10^6}{16406699.844} = 0.06095 \cong 6.1\ cm$$
$$u_m = \frac{6104456.248}{10^6} = 6.10446 \cong 6.1\frac{m}{s}$$

We can perform a check on these dimensions by falling back on the power-mass flow rate equation.

$$q_m = 59955\dot{m}_m \rightarrow \dot{m}_m = \frac{10^6}{59955} = 16.6792 \cong 16.7\frac{kg}{s}$$
$$\dot{m}_m = \overline{\rho_m} A_m u_m = \overline{\rho_m}\frac{\pi D_m^2}{4} u_m = (936.442)\left(\frac{\pi}{4}\right)(0.06095)^2(6.10446) = 16.679 \cong 16.7\frac{kg}{s}$$

2.2.4 Heater Analysis

To continue on to the length and time scaling analysis, the dynamics of the heater section must be analyzed; its results will determine the desired geometry of the heater, and thus the desired length ratios between model and prototype components.

---

10. Greene, Sherrell R., et al., "Pre-conceptual Design of a Fluoride-Salt-Cooled Small Modular Advanced High-Temperature Reactor (smAHTR)," Oak Ridge National Laboratory, ORNL/TM-2010/199, December 2010.
11. Jianjun, Zhou, et al., "The influence of lower plenum and distribution plates to thermal hydraulics characteristics of MSRs," Nuclear Engineering and Design, Vo. 256. 2013, p. 235–248.
12. Cammi, Antonio, et al., "A multi-physics modeling approach to the dynamics of Molten Salt Reactors," Annals of Nuclear Energy, Vo. 38, 2011, p. 1356-1372.
13. Xiao, Yao, et al., "Numerical analysis for a molten salt reactor in the presence of localized perturbations," Progress in Nuclear Energy, Vo. 60, 2012, p. 61–72.
14. Avigni, P. and B. Petrovic, "Fuel element and full core thermal-hydraulics analysis of the AHTR for the evaluation of the LOFC transient," Annals of Nuclear Energy, 2013 (In Press).

This analysis assumes that the heat source for the experiment will be a resistive heater.

Prior to selecting a material for resistive heating, one can derive certain relations to better understand the range of length and cross section. In addition, the Nusselt number and heat transfer coefficient can also be derived without settling on all aspects of the heater geometry.

In particular, analyzing the heater characteristics will give us a better understanding of the length and time scaling for the scaled experiment.

Unless otherwise specified, all equations in this section were taken from Incropera and Dewitt 2011.[15]

The average Reynolds number in the primary leg is:

$$Re = \frac{uD}{\nu} = \frac{(6.1)(0.061)}{5.23787 * 10^{-7}} = 710403 \sim 7.1 * 10^5$$

This allows us to use the Gnielinski correlation for the Nusselt number for turbulent pipe flow:

$$Nu_D = \frac{\left(\frac{f}{8}\right)(Re - 1000)(\mathrm{Pr})}{1 + 12.7\left(\frac{f}{8}\right)^{\frac{1}{2}}\left(Pr^{\frac{2}{3}} - 1\right)}$$

f is the friction factor, found by the Petukhov correlation for turbulent flow in a smooth surface.

$$f = (0.79\ln(Re) - 1.64)^{-2}$$

To properly characterize the thermophysical and heat transfer properties of the heater section, the different values must analyzed with respect to Dowtherm's temperature range, $156 - 186°C$. Table 9 lists the values at these two temperatures.

Table 9. Properties necessary for model heater characterization.

Temperature	156°C	186°C
Kinematic Viscosity [m^2/s]	$5.89075 * 10^{-7}$	$4.80658 * 10^{-7}$
Thermal Conductivity [W/m-K]	0.11704	0.11224
Reynolds Number	631668	774147
Prandtl Number	9.25958	7.94015
Friction Factor	0.012593	0.01215
Nusselt Number	3382.08	3767.18
Heat Transfer Coefficient [W/m^2-K]	6489.15	6931.62

Now, we turn to the heat transfer relations that govern conduction in a cylindrical system; specifically, the equation that relates the heat transfer coefficient, volumetric heat generation, radius, and temperature. Figure 6 shows a diagram that clarifies the locations of the variables.

15. Incropera, Frank P. and David P. Dewitt, "Fundamentals of Heat and Mass Transfer," *7th Edition*, John Wiley and Sons, Hoboken, New Jersey, 2011.

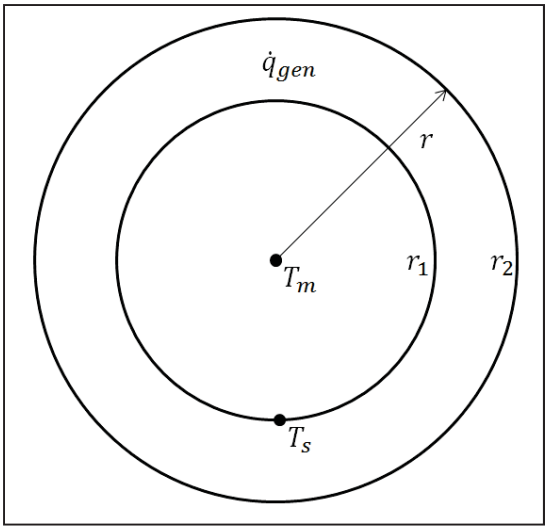

Figure 6. Cross section of the heater pipe and the locations of the relevant variables.

$$h = \frac{\dot{q}(r_2^2 - r_1^2)}{2r_1(T_s - T_m)}$$

The volumetric heat generation rate is unknown; however, we do know the total energy production rate and the theoretical volume. The total energy production and the theoretical volume can be used to derive the volumetric heat generation rate.

$$\dot{q} = \frac{\dot{E}}{\pi(r_2^2 - r_1^2)L} \rightarrow\ h = \frac{\dot{E}}{\pi(r_2^2 - r_1^2)L}\frac{(r_2^2 - r_1^2)}{2r_1(T_s - T_m)} = \frac{\dot{E}}{2r_1\pi L(T_s - T_m)}$$

A relation can then be derived that gives the temperature of the inner surface as a function of the total length of the heating element.

$$T_s(x) = T_m(x) + \frac{\dot{E}}{2r_1\pi Lh} = \frac{10^6}{0.061\pi Lh(x)}$$

The values for heat transfer coefficient and fluid temperature at $x = 0$ and $x = L$ correspond to the minimum and maximum temperatures of Dowtherm. Thus:

$$T_s(x = 0) = 156 + \frac{10^6}{0.061\pi L(6489.15)} = 156 + \frac{804.142}{L}$$
$$T_s(x = L) = 186 + \frac{10^6}{0.061\pi L(6931.62)} = 186 + \frac{752.81}{L}$$

Figure 7 shows the temperature rise along the heater pipe's inner diameter (T_s) and the mean fluid temperature (T_m), assuming a 6 m core height.

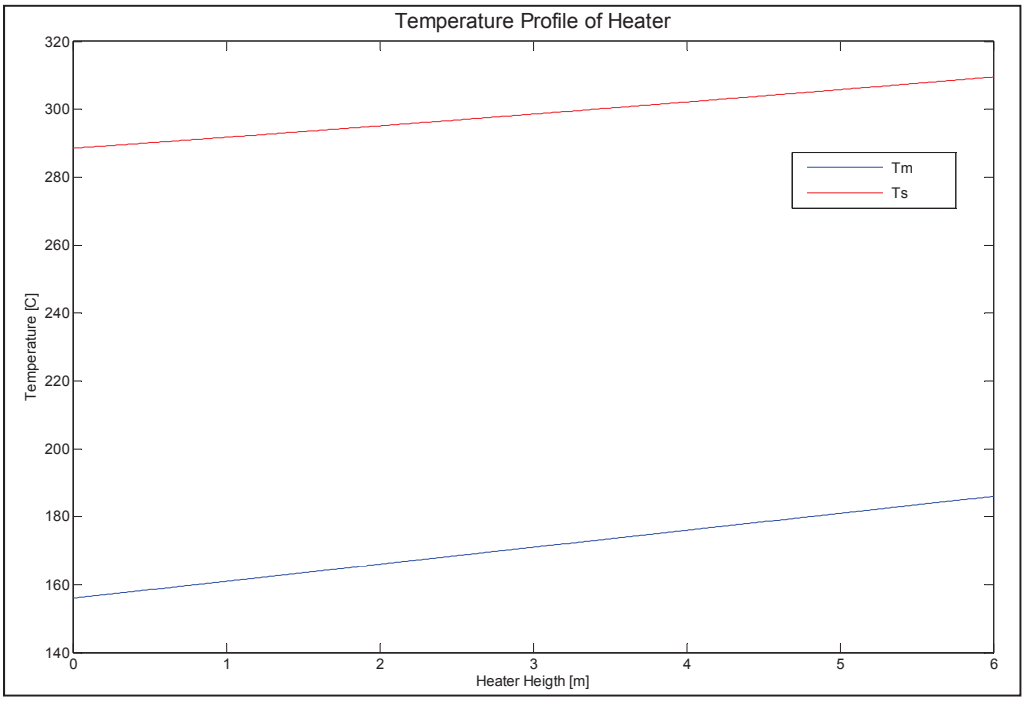

Figure 7. Graph of the mean and surface temperatures of the heater, as a function of height.

The longer the heating element, the lower the inner surface temperature will be. Thus, the optimal design will make the heating element as long as the facility's restrictions will allow for, so as to minimize stress on the heater material.

2.2.5 Analysis of the Length and Time Ratios

The values of the general prototype lengths can be derived from the pre-conceptual design of the smAHTR. Figure 8 shows a diagram of the smAHTR and its dimensions, and Table 10 shows the specific dimensions that will be used for scaling. The thermal height is the distance between the center of the core and the center of the heat exchanger.

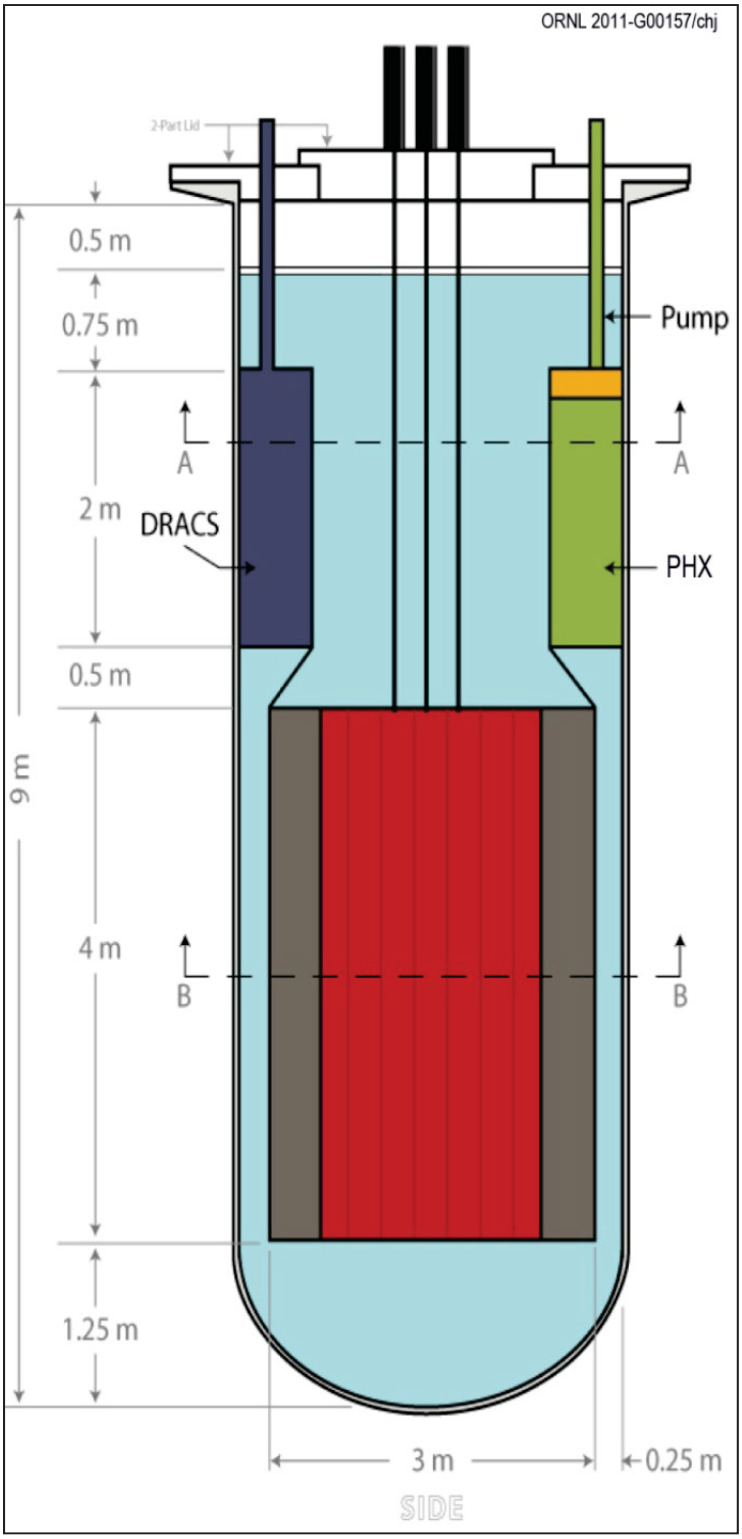

Figure 8. Diagram of the smAHTR's geometry.

Table 10. Values for the prototype's length parameters.

Parameter (Prototype)	Value
Core Height	$4\ m$
Thermal Height	$3.5\ m$
Total Height	$6.5\ m$
Horizontal Distance	$1.625\ m$

The expected allotment of space at the Energy Systems Laboratory (ESL) will be a 25 ft × 25 ft footprint, with a height of 40 ft. This corresponds to a 7.62 m × 7.62 m × 12.2 m volume. Therefore, the heights and lengths of the experimental facility's components can be larger than the prototype, which allows for a less distorted time ratio. If a maximization of the length ratio is the goal, then the model to prototype length proportion can be 1.5. Table 11 shows the resulting lengths of the model's components.

Table 11. Values for the model's length parameters.

Parameter (Model)	Value
Core Height	$6\ m$
Thermal Height	$5.25\ m$
Total Height	$9.75\ m$
Horizontal Distance	$2.4375\ m$

Thus, we can now also find the residence time ratio (the time that the working fluid spends in a component) using the core size as a baseline:

$$\frac{\frac{l_{0,m}}{u_{0,m}}}{\frac{l_{0,p}}{u_{0,p}}} = \frac{\frac{6}{6.1}}{\frac{4}{1}} = 0.245902$$

2.2.6 Theoretical Pressure Drop and Pump Power

It is important to estimate the pressure drop across the entire loop, so as to baseline a minimum value for the pump power. Using the pressure drop equation for pipe flow given in Incropera:

$$\Delta p = f\frac{\rho u^2}{2D}(x_2 - x_1)$$

Here $(x_2 - x_1)$ refers to the total length of the loop. Since the loop is a rectangle, we can find this value by multiplying the heights and horizontal distance by two and adding the values together. This value is:

$$9.75 * 2 + 2.4375 * 2 = 24.375\ m$$

The friction factor is found using the average Reynolds number of the loop:

$$f = (0.79\ln(Re) - 1.64)^{-2} = (0.79\ln(710403) - 1.64)^{-2} = 0.012334$$

Thus, the pressure drop is found:

$$\Delta p = (0.012334)\frac{(936.442)(6.1^2)}{2 * 0.061}(24.375) = 85867.6\ Pa \approx 86\ kPa$$

We can use this to determine the necessary pump power for the loop:

$$P = (\Delta p)\dot{\forall} = \frac{(\Delta p)\dot{m}}{\rho} = \frac{(85867.6)(16.7)}{936.442} = 1531.32\ W \approx 1.5\ kW$$

Thus, a $2\ kW$ pump should be more than sufficient to drive the flow of the loop.

2.3 Scaling Results

The results of the scaling analysis are shown in Table 12. A diagram of the experiment is shown in Figure 9.

Table 12. Model and prototype parameters and resultant model-to-prototype ratios.

Parameter	Prototype	Model	Model-to-Prototype Ratio
Working Fluid	Flibe	Dowtherm A	n/a
Prandtl Range	$[9.27, 7.93]$	$[9.26, 7.94]$	n/a
T_{min}[°C]	800	156	n/a
T_{max}[°C]	850	186	n/a
ΔT[K]	50	30	0.6
Power [MWth]	300	1	$0.00\overline{3}$
Diameter [m]	1.25	0.061	0.0488
Velocity $[\frac{m}{s}]$	1	6.1	6.1
Mass Flow $\left[\frac{kg}{s}\right]$	2485	16.7	0.00672
Average Reynolds	707590	710403	1.00398
Average Friction Factor	0.012343	0.012334	0.999304
Average Nusselt	3612.69	3625.73	1.00361
Core Height [m]	4	6	1.5
Thermal Height [m]	3.5	5.25	1.5
Horizontal Distance [m]	1.625	2.4375	1.5
Total Height [m]	6.5	9.75	1.5
Residence Time [s]	4	0.9836	0.2459

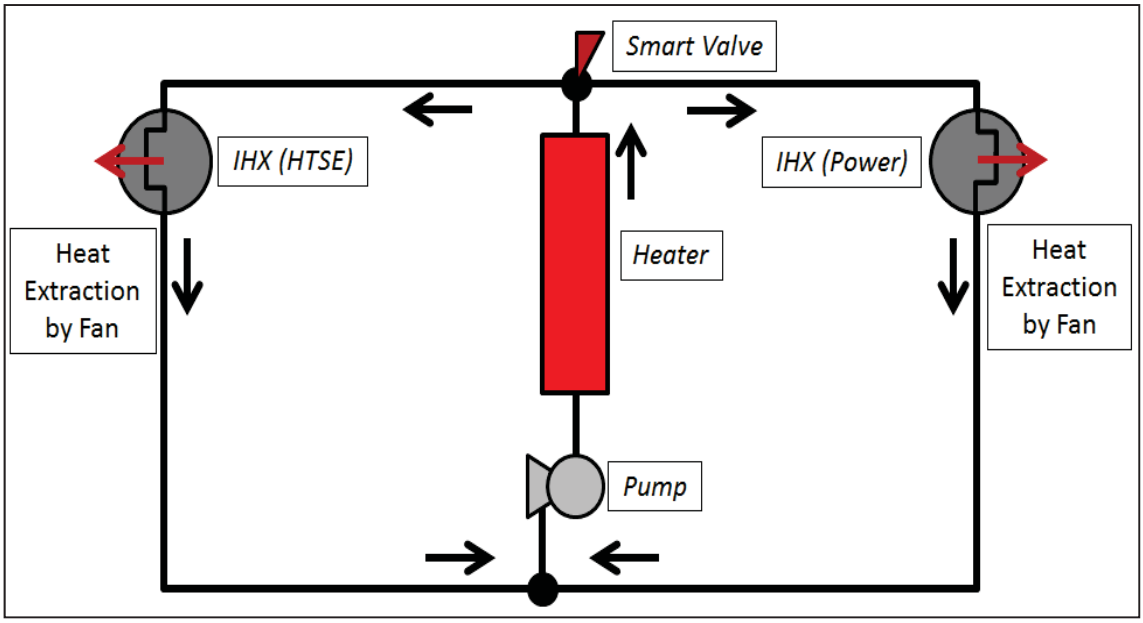

Figure 9. Diagram of the scaled facility and primary subcomponents.

2.4 Discussion of Limitations and Alternative Approaches

While scaling the Reynolds number is effective for matching the prototype's flow regime and friction factor, the residence time is skewed. As Subsection 2.2.5 points out, the residence time of the scaled facility is approximately one-fourth of the residence time of the prototype; this poses challenges when attempting to use the facility to analyze fluid transients and control couplings.

One simple solution could be to simply turn down the flow velocity in the primary leg to $1.5\frac{m}{s}$, which would make the residence time ratio between the prototype and the model equal to unity. However, this would this would result in a smaller Reynolds number (174689, as opposed to 710403, a 75% decrease), and have a corresponding impact on the friction factor and Nusselt number. Therefore, the choice to take this simple strategy to scale the residence time is contingent on the specifics of the required analysis—it would be inadvisable if a particular experiment requires a properly scaled friction factor.

3. Analysis of Prototype Interconnections and Control

To understand the control dynamics of the scaled facility, it is necessary to analyze the control dynamics of the prototype facility. Specifically, we must examine the way heat and power flow is affected by changes in various system parameters—especially changes in grid demand, since the ultimate purpose of an FHR-HTSE system is to be load-following.

The main components of this system are listed below. Figure 10 shows the interconnections of the components, where red signifies a thermal energy transfer, and black signifies an electrical energy transfer.

- Reactor
- HTSE
- Power Block (Supercritical CO_2 Loop)
- Power Control
- Energy Storage (Thermal and Electrical)
- Renewable Power Generator (Wind or Solar).

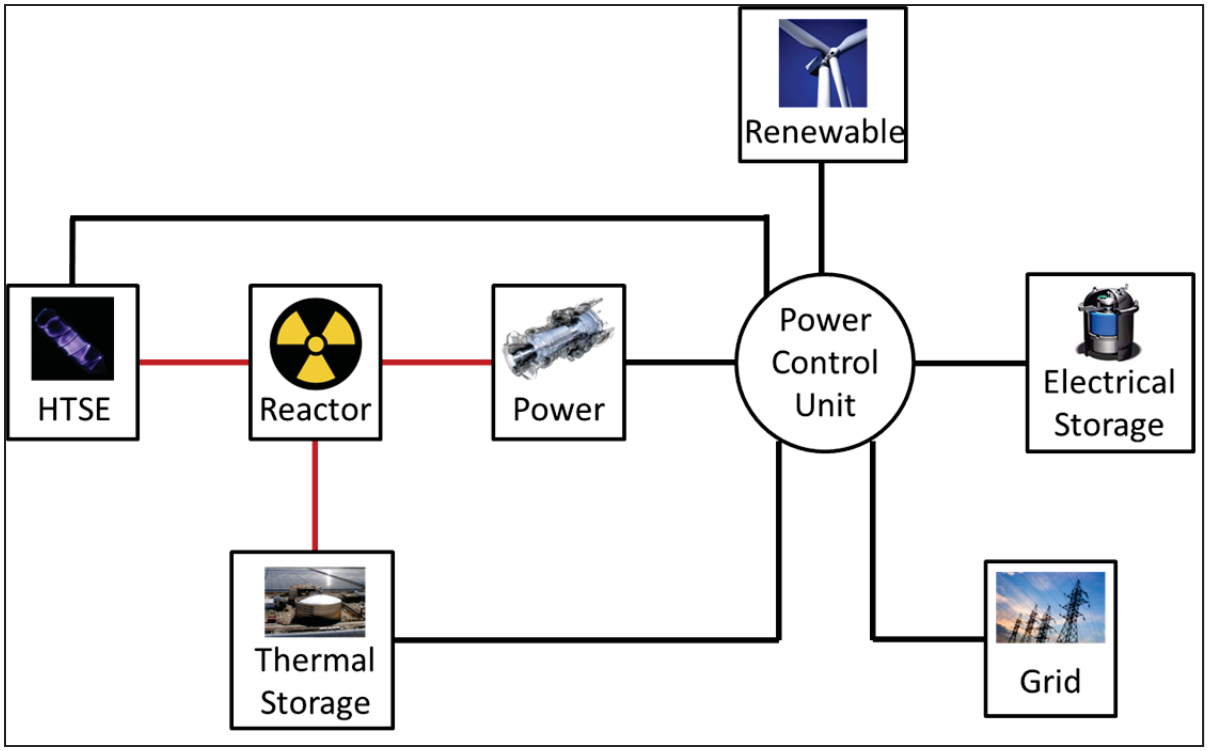

Figure 10. Diagram of major FHR-HTSE components.

3.1 Prototype Interconnections—Thermal Energy Flow

The lists below describe the various hardware and subcomponents that must be in place between the primary components that moderate the thermal energy flow. The subcomponents are listed in roughly the order in which they are encountered by the heat flow. Table 13 shows the interconnections between the reactor and the two main intermediate loops and their respective processes.

Table 13. Interconnections between reactor and the two thermal-based processes.

Reactor-HTSE	Reactor-SCO_2
Smart Valve	Smart Valve
Pipe (Flibe)	Pipe (Flibe)
Heat-Exchanger (Salt-Helium)	Heat-Exchanger (Salt-Salt)
Pipe (Helium)	Pipe (KF-ZrF_4)
Compressor	Pump
Heat-Exchanger (Helium-Water)x2	Heat-Exchanger (Salt-CO_2)

It is also necessary to analyze the interconnections between the reactor and the thermal energy storage. These connections depend on the specific type of thermal energy storage. It seems that the preferred system would be a molten-salt system. Table 14 shows the interconnections between the reactor and the thermal energy storage system, and the interconnections between the storage and the power generation system.

Table 14. Interconnections between the reactor, thermal energy storage system, and the power generation unit.

Reactor-Thermal Storage	Thermal Storage-Power Generation
Smart Valve	Pipe (Storage system's working fluid)
Pipe (Flibe)	Heat-Exchanger (Salt-Water/Steam)
Heat-Exchanger (Salt-Salt)	Steam Generator
Pipe (Storage system's working fluid)	

The complexity with the thermal energy storage is that there is no clear design as to how to incorporate this loop into the existing two-flow primary loop. A third flow-path, moderated by a fluidic diode, could be a possible item to add to render feasible a connection between the primary loop and the molten-salt thermal storage system.

It might also be fruitful to explore the possibility of connecting this end of the thermal energy storage system directly with the supercritical CO_2 block, so to not invest money into a second turbine system.

3.2 Prototype Interconnections—Electrical Energy Flow

There is not much available for major interconnections between the power-based components, other than the actual power control unit. We can divide the couplings with the power control unit into inputs and outputs. Inputs signify sources from which power is drawn; outputs signify sources that consume power. Table 15 and Figure 11 show the inputs and outputs of the power control unit in a table and a graphical form, respectively.

Table 15. List of inputs and outputs to the power control module.

Inputs	Outputs
SCO2 (Power Cycle)	HTSE
Renewable Generation	Grid
Electrical Storage System	Electrical Storage System
Thermal Storage System	

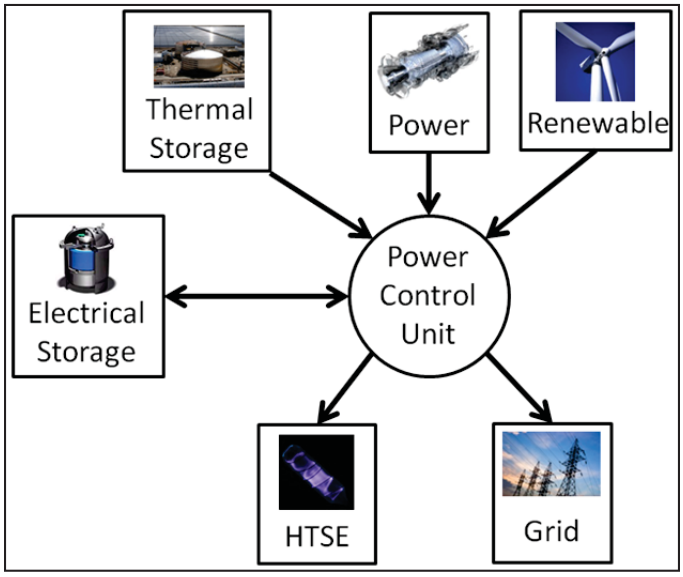

Figure 11. Diagram of inputs and outputs to the power control unit.

The necessity of the electrical storage system (i.e., flywheel) is uncertain. It depends on the transients associated with attempting to have the system follow the load, simultaneously with prioritizing renewable power transmission to the grid. If the rest of the system's components (mainly the power block and the HTSE) cannot effectively cycle up and down based on grid demand, then an electrical storage system may be necessary to provide an additional buffer.

3.3 Analysis of Component Dependence on Thermal Heat Flows

It is necessary to examine the relationships between the components to understand the control algorithms that will govern the system response to changes in grid demand and renewable energy generation. Table 16 lists the values of key components when the total power output to the grid is at three different values. These values were calculated using ASPEN models specified in Wood and McKellar[16] and Bragg-Sitton et al. (see Table 16). All values, unless otherwise specified, are in megawatts.

Table 16. Values of thermal and electrical energy transfers as a function of system output to grid (derived from ASPEN codes).

	Net Output to Grid		
Subsystem	0 MW	70 MW	100 MW
Q_HTSE [MWth]	33.6	17.9	11.1
Q_Power [MWth]	266.4	282.2	288.9
P_Circs [MWe]	7.2	3.8	2.4
P_HTSE [MWe]	125.4	66.6	41.4
P_Power [MWe]	72.3	76.6	78.4
P_Cooling [MWe]	0.5	0.4	0.4
Ptot_Use [MWe]	205.3	147.5	122.7
Power_Gen [MWe]	205.3	217.5	222.7
H_Produced [kg/s]	1.013	0.538	0.335

The "Qs" stand for the heat flow to either the power cycle or the HTSE loop. The "Ps" stand for the power consumed by four different components: the circulators for the primary and secondary loops, the HTSE, the power cycle, and the cooling towers.

A key relationship to consider is that between power output to the grid and the heat flow dynamics of the primary loop. This relation is more complicated than a typical non-hybrid reactor because the HTSE demands both power and heat inputs, and there is a set relationship between the power and heat inputs (that is, sending a certain amount of heat to the HTSE requires a certain amount of power to be sent to the HTSE as well, if all the heat is to be used to produce hydrogen).

To find this relation, we begin with the following:

$$P_{out} = P_{gen} - P_{use}$$

As mentioned previously, there are four primary points of power consumption within the system. Inserting these into the relation:

$$P_{out} = P_{gen} - (P_{circ} + P_{HTSE} + P_{power} + P_{cool})$$

The power consumed by the four components can be put in terms of the heat flow to the HTSE, Q_{HTSE}, by examining the values given in the table above, as well as the aforementioned ASPEN models.

16. Wood, R. A. and M. G. McKellar, "Hydrogen Production via FHR-Integrated High-Temperature Steam Electrolysis," Idaho National Laboratory, TEV-1776, March 2013.

3.3.1 Loop Circulation

The power consumed by the primary and secondary loop circulation is dominated by the compressor on the HTSE. As such, it is a function of the mass flow rate of the HTSE loop, which itself is a function of the heat input. Table 17 shows the heat input, compressor input, and work-to-heat input ratio.

Table 17. HTSE compressor power consumption dependence on heat flow to the HTSE loop.

Net Output [MWe]	Qh [MWth]	Wc [MWe]	Wc/Qh [MWe/MWth]
0	33.6	7.158	0.213036
70	17.9	3.804	0.212514
100	11.1	2.366	0.213153
		Average	0.212901

We can use the emergent linear relation to put the power consumption for loop circulation in terms of the heat input to the HTSE:

$$P_{circ} = 0.213 Q_{HTSE}$$

3.3.2 HTSE

Next, we analyze the power consumption by the HTSE as a function of the heat input. Table 18 below takes the relevant values from the Table 16 to find the power-heat proportion.

Table 18. HTSE power consumption dependence on heat flow to HTSE loop.

Net Output [MWe]	Qh [MWth]	Phtse [MWe]	Phtse/Qh [MWe/MWth]
0	33.6	125.4	3.732143
70	17.9	66.6	3.72067
100	11.1	41.4	3.72973
		Average	3.727514

Thus:

$$P_{HTSE} = 3.728 Q_{HTSE}$$

3.3.3 Power Cycle

Again taking relevant values from the Table 16, Table 19 documents the power consumption of the power cycle as a function of grid demand and heat flow to the HTSE loop.

Table 19. Power cycle power consumption dependence on heat flow to HTSE loop.

Net Output [MWe]	Qp [MWth]	Ppow [MWe]	Ppow/Qp [MWe/MWth]
0	266.4	72.3	0.271396
70	282.2	76.6	0.271439
100	288.9	78.4	0.271374
		Average	0.271403

This data is slightly different from the preceding tables, as it takes the value of the heat input to the power cycle, rather than the HTSE cycle. Thus, we find a relation between the power consumption and heat input to the power cycle, which can then be written in terms of the heat input to the HTSE loop:

$$P_{power} = 0.271Q_{power} = 0.271(300 - Q_{HTSE}) = 81.3 - 0.271Q_{HTSE}$$

3.3.4 Cooling Towers

The power consumption by the cooling towers is divided between a pump and a compressor. Table 20 below takes values from the ASPEN flow sheets and provides the pump and compressor power consumptions for each value of net power output.

Table 20. Cooling tower power consumption dependence on net system output to grid.

Net Output [MWe]	Pump [MWe]	Compressor [MWe]	Total [MWe]
0	0.229	0.226	0.455
70	0.226	0.222	0.448
100	0.225	0.221	0.446
		Average	0.449667

The power consumption by the cooling towers is essentially constant. Thus:

$$P_{cool} = 0.45\ MWe$$

3.3.5 Power Generation

The power generation term can be found by examining the proportion of heat input to the power cycle that is converted to electricity. Table 21 shows this dependence.

Table 21. Power generation dependence on heat flow to power loop.

Net Output [MWe]	Qp [MWth]	Pgen [MWe]	Pgen/Qp [MWe/MWth]
0	266.4	205.3	0.770646
70	282.2	217.5	0.77073
100	288.9	222.7	0.770855
		Average	0.770744

Thus:

$$P_{gen} = 0.771Q_{power} = 0.771(300 - Q_{HTSE}) = 231.3 - 0.771Q_{HTSE}$$

3.3.6 Relations of Net Power Output and Thermal Energy Flows

We can insert these new equations back into the original relation for power output:

$$\begin{gathered} P_{out} = P_{gen} - (P_{circ} + P_{HTSE} + P_{power} + P_{cool}) \\ = P_{gen} - (0.213Q_{HTSE} + 3.728Q_{HTSE} + (81.3 - 0.271Q_{HTSE}) + 0.45) \\ = P_{gen} - (3.67Q_{HTSE} + 81.75) \end{gathered}$$

Inserting the power generation term into the equation of total power output:

$$P_{out} = (231.3 - 0.771Q_{HTSE}) - (3.67Q_{HTSE} + 81.75)$$

$$P_{out} = 149.55 - 4.441Q_{HTSE}$$
$$P_{out} = 4.441Q_{power} - 1182.75$$

These relations are useful because it allows the system operator to predict how much thermal energy has to be sent to each of the process loops for a given value of net electrical output to the grid. Figure 12 shows this in a graphical form.

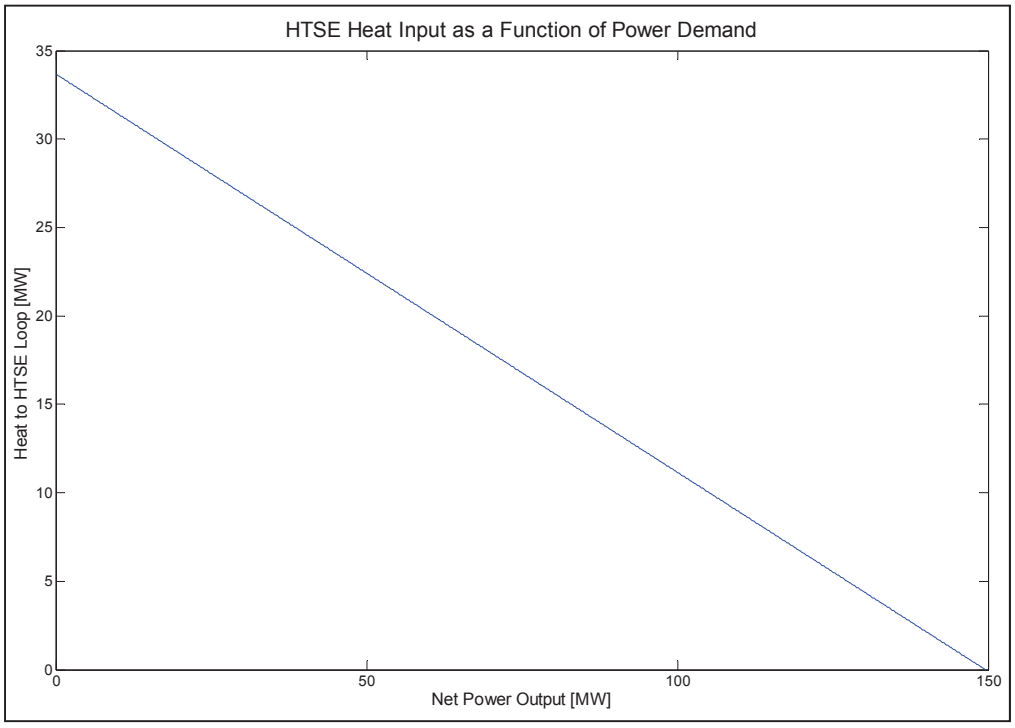

Figure 12. Graph of the dependence of heat flow to the HTSE loop on the required net electrical generation of the system.

3.4 Open-Loop Control Logic

The control system for the prototype facility has to be based on set-points being dynamically set by an open-loop algorithm. The primary measured variable that determines the set-points for the primary and secondary loop controllers is the power demand from the power control unit. This value will be proportional to the power demand from the grid, since the overall system's purpose is to be load-following. Figure 13 shows a diagram of the proposed control hierarchy.

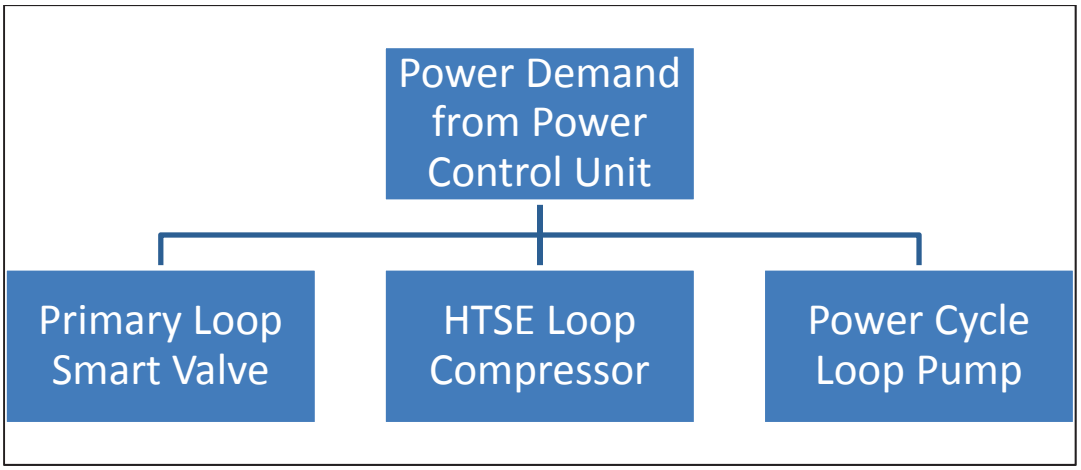

Figure 13. Open-loop control hierarchy for the prototype system.

This proposed hierarchy also makes clear the specific points of analysis that have to be performed in order to have a functioning control system. It will be necessary to analyze the response times of the smart valve, compressor, and pump, as well as the time it takes for a shift in the smart valve to result in a shift in the heat load to the secondary loops.

3.4.1 Open-Loop Control of Primary Loop Smart Valve

The primary loop mass flow rate is controlled by the smart valve, which splits the primary leg flow into two directions: one toward the salt-salt heat-exchanger (which delivers heat to the power cycle) and the other toward the salt-helium heat-exchanger (which delivers heat to the HTSE).

To find this relation, we can simply invert the power-heat equations given above (it should be noted that the numerator dimensions are MWe, and the denominator dimensions are $\frac{MWe}{MWth}$):

$$Q_{HTSE} = \frac{P_{out} - 149.55}{-4.441}$$
$$Q_{power} = \frac{P_{out} + 1182.75}{4.441}$$

These equations tell us the dynamics of the smart valve at the top of the primary leg that splits the core outlet flow. Higher power demand requires the smart valve to send more mass flow toward the power cycle, and lower power demand requires the smart valve to send more mass flow toward the HTSE. If we assume that the smart valve operates in terms of the mass flow fraction directed toward the power loop, then we can divide the second equation to get a relation between mass flow fraction and required power. Figure 14 shows this relation in a graphical form.

$$\dot{m}_{\%,power} = \frac{P_{out} + 1182.75}{4.441 * 300[MWth]} = \frac{P_{out} + 1182.75}{1332.3}$$

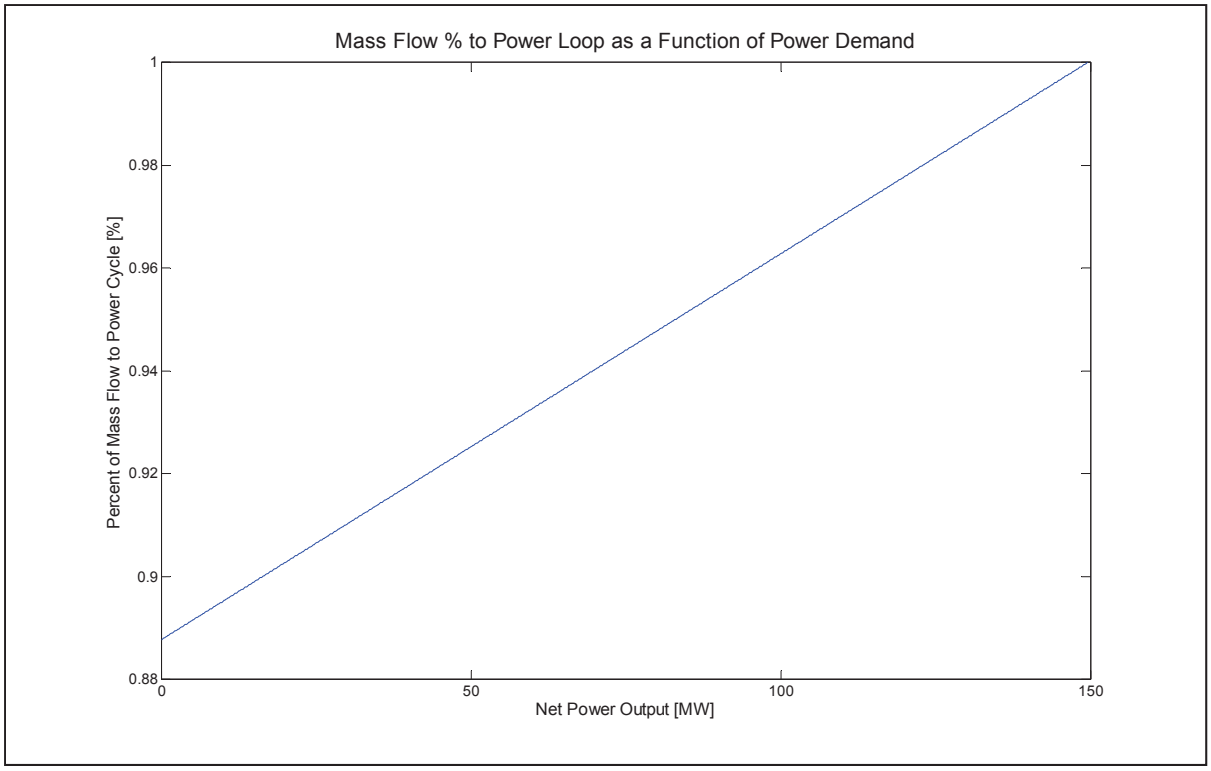

Figure 14. Graph of the proportion of heat from the reactor that is sent to the power cycle, as a function of the system's net power output.

3.4.2 Open-Loop Control of HTSE Loop Compressor

The mass flow rate of the HTSE loop is controlled by a compressor. To control the compressor using the value of the power demand, we insert the HTSE heat-power demand relation into the compressor-HTSE heat equation. It should be noted that in the value of 0.213 has the dimensions of $\frac{MWe}{MWth}$, and thus cancels out with the dimensions of the value of -4.441.

$$P_{circ} = W_c = 0.213 Q_{HTSE} = (0.213)\left(\frac{P_{out} - 149.55}{-4.441}\right) = \frac{P_{out} - 149.55}{-20.85}$$

To control the compressor using the smart valve, we can insert the mass flow fraction-power relation into the above equation.

$$P_{out} = 1332.3\dot{m}_{\%,power} - 1182.75$$

$$W_c = \frac{P_{out} - 149.55}{-20.85} = \frac{(1332.3\dot{m}_{\%,power} - 1182.75) - 149.55}{-20.85} = 63.899(1 - \dot{m}_{\%,power})$$

3.4.3 Open-Loop Control of Power Cycle Loop Pump

The resolution of the relationship between Q_{power} and the pump power on the power cycle loop in the ASPEN code is too low for us to derive any useful linear relation. Between a power output of 0 MW and 100 MW, the pump power is between 8 kW and 9 kW. Thus, it will be sufficient to set the initial pump power value to 8.5 kW, and allow a feedback control algorithm to fine-tune the power during operation.

$$P_{pow,pump} = 8.5 * 10^{-3}\ MWe$$

4. Analysis of Model Interconnections and Control

Using a methodology identical to the one used to analyze the prototype control dynamics, we can examine the proportions between the heat flows in the primary loop and the power consumption by the four primary components. This allows us to find a direct relation between the heat flows and the power output of the system. The governing equations of the subcomponents are mostly identical between the prototype and the model, since they are in terms of proportions. The only equation that changes is the governing equation for the power consumption by the cooling towers (translating this equation is done simply by dividing by the quotient of the thermal powers' of the prototype and the model, since it is assumed that the amount of energy extracted by the cooling towers is proportional to a given system's total thermal energy production).

The following equations relate the primary leg heat flows to the consumption of power by the HTSE loop compressor, the HTSE, the power cycle, and the cooling towers, respectively. It should be noted that as opposed to Section 3, the following equations are in terms of watts, not megawatts (hence the 10^6 term in in power cycle consumption equation, which relates to the $1\ MWth$ thermal energy generation of the scaled facility).

$$P_{circl} = 0.213 Q_{HTSE}$$
$$P_{HTSE} = 3.728 Q_{HTSE}$$
$$P_{power} = 0.271 Q_{power} = 0.271(10^6 - Q_{HTSE})$$

$$P_{cool} = \frac{0.45}{300} = 0.0015\ MW = 1500\ W$$

We also know the relation between power generation and heat sent to the power loop:

$$P_{gen} = 0.771 Q_{power} = 0.771(10^6 - Q_{HTSE})$$

We can thus find the final power output with the following relation (units in watts):

$$\begin{aligned} P_{out} &= P_{gen} - P_{cons} \\ &= 0.771(10^6 - Q_{HTSE}) - (0.213 Q_{HTSE} + 3.728 Q_{HTSE} + 0.271(10^6 - Q_{HTSE}) + 1500) \\ &= -4.441 Q_{HTSE} + 498500 = 4.441 Q_{power} - 3942500 \end{aligned}$$

4.1 Hardware and Instrumentation Needs and Recommendations

Before proceeding with the quantitative analysis of the relationship between the scaled model's subcomponents, it is necessary to clarify the ways in which the prototype components will be scaled and simulated in the scaled facility. This section also recommends instrumentation, and gives a brief discussion on some of the phenomena that the specific instruments will be used to measure and analyze.

4.1.1 Power Supply

As laid out in Section 2.2, the preliminary scaling analysis suggests that the thermal system requires a $1\ MW$ power supply that can be efficiently converted into heat to mimic the heat that would be generated by an operating reactor. It is currently anticipated that resistive heating (Joule heating) will be used; that is, the control system will be designed to send time-varying current to an electrical heater or bank of heaters based to vary the "reactor" power based on the system requirements. This heater control will drive thermal energy generation into the system.

4.1.2 Flow Control

Several components are required to interact with the flow dynamics of the facility.

- Pump: Scaling analyses indicate a need for a 2 kW pump is needed to overcome the expected loop pressure drop.
- Flow-meter: A device that can measure the working fluid mass flow rate and velocity is needed at three separate points in the facility: the primary leg, the power cycle leg, and the HTSE leg.
- Smart Valve: A programmable, dynamic smart valve is needed to moderate flow separation at the top of the primary leg to properly apportion the thermal energy to simulate the dynamic nature of the hybridized system. The smart valve will need to continuously actuate in response to data that simulates the variation in required power generation. The associated control system will be designed to limit the variability as a function of time to avoid constant fluctuations.

4.1.3 Heat-Exchangers

At this initial stage of development for the scaled facility, it is assumed that the intermediate loops will be simulated with hardware and software, rather than be scaled like the primary loop was. However, this still leaves open the possibility of future scaling analysis to be done, that could replace the hardware-software simulation currently proposed with an actual physical model.

There are two components needed to interact with the points of heat exchange in the primary loop.

- Fan: The IHXs for the power cycle loop and the HTSE loop can be simulated with a fan. The heat extraction from the fan simulates the heat extraction from the primary loop into the heat exchanger and the secondary loop.
- Variable Speed Drive (VSD): A VSD actuates the fan speed in response to the required heat extraction needed at a given time. The VSD can be controlled remotely from a computer via a USB-485 cable.

4.1.4 Thermocouples

Thermocouples will be needed to measure temperature at various points in the loop. Ideally there will be several thermocouples at each measurement point to mitigate measurement discrepancies, radial variation, and thermocouple failure. Important points of measurement are before and after the heater (reactor simulator), smart valve, IHXs, and pump. The thermocouples are connected to a digital reader, which can then relay this information to the controller. These "state estimators" will be used in the control system logic that drives the individual component settings.

Thermocouples should be placed in locations before and after heat transfer takes place, and directly within the area of heat transfer, when possible. Figure 15 shows the proposed locations for thermocouples within the simplified thermal generation loop.

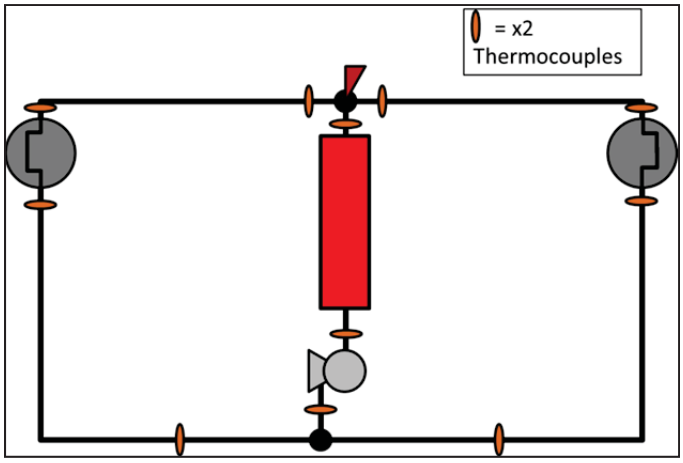

Figure 15. Diagram of proposed thermocouple locations around the loop.

It is also desirable to place thermocouples along the heater component (reactor simulator) to properly characterize the heater temperature profile and to provide state estimation for optimal control that emulates the expected reactor behavior. Figure 16 shows the proposed locations for thermocouples in the heater region. The light brown area signifies insulation around the heater to measure heat loss from the heater component. The gray area signifies the resistive heater. This diagram assumes a simplified configuration with a single heater element, but heating alternately may be implemented using a bank of heaters to meet the appropriate power and temperature profiles. Thermocouples cannot be in direct contact with the resistive elements; instead, they should be located along the inner wall as close to the heating element as possible (or should be attached to the sheath around the element if one exists). Specifics of the thermocouple layout within heating element or elements can only be refined after the elements have been selected from available off-the-shelf components or designed specifically for this application.

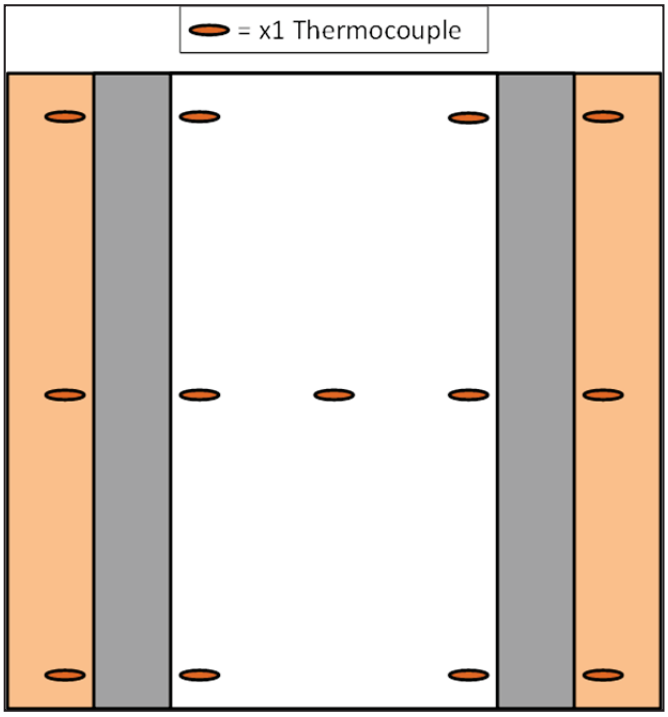

Figure 16. Diagram of proposed thermocouple locations in the heating section.

4.1.5 Pressure Transducers

Pressure transducers that can operate at the high system temperatures will be needed to analyze the pressure drop at various points in the loop.

4.2 Analysis of Control Algorithms for the Scaled Facility's Subcomponents

4.2.1 Control of the Smart Valve

The smart valve that splits the flow from the primary leg into two flows—one to the power cycle, another to the HTSE loop—will have an initial value set by the power demand.

Inverting this equation, and dividing by the total power of the facility ($1\ MW = 10^6\ W$), we can obtain the equation that relates the mass flow to the power loop as a function of required power output.

$$Q_{power} = \frac{P_{out} + 3942500}{4.441} \rightarrow \dot{m}_{\%,power} = \frac{P_{out} + 3942500}{4441000}$$

Figure 17 shows this linear relationship between the percent of mass flow to the power loop, as a function of net power output.

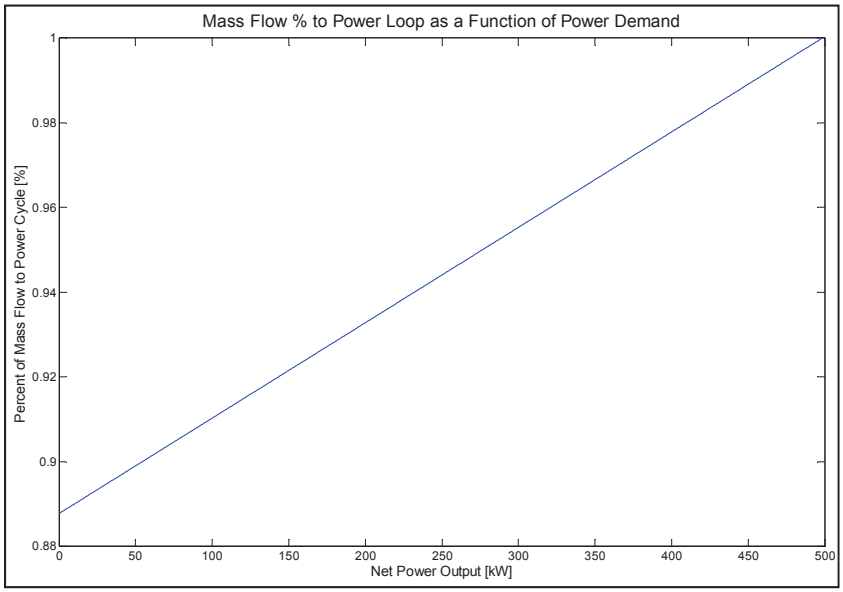

Figure 17. Graph of the percentage of primary leg flow that is sent to the power loop in the scaled facility, as a function of net system electrical output.

While the set-point will be determined from the given equation, feedback control is necessary to manage any disturbances and errors. Feedback control for the smart valve will take measurements from the flow meter on the power loop to determine the incremental change in value for the smart valve position.

4.2.2 Control of the Intermediate Heat Exchangers

In the preliminary simplified design of the scaled facility the IHXs are simulated using fans to extract heat from the primary loop. The fans are controlled by VSDs that change fan speeds—and thus, heat extraction rates—by varying the frequency in response to signals from the controller.

The required heat extraction rates are identical to the heat flows previously analyzed.

$$IHX_{power} = Q_{power} = \frac{P_{out} + 3942500}{4.441}$$
$$IHX_{HTSE} = Q_{HTSE} = \frac{P_{out} - 498500}{-4.441}$$

Feedback control for the VSDs will take the temperature of the primary loop fluid (note that FLiBe may be simulated using Dowtherm) after it leaves the heat exchanger, and accordingly increase or decrease the fan speeds to achieve the required temperature.

4.2.3 Control of the Primary Loop Pump

The pump is located on the primary leg upstream of the heater section. It will run at a constant power (~1.5 kW) to maintain the flow rate through the primary leg (preliminary analysis indicate that the mass flow rate will be 16.7 kg/s). To stabilize at the required mass flow rate, feedback control based on measurements from the primary leg's flow-meter will be used to regulate the specific power value of the pump.

4.2.4 Control of the Heater

Preliminary analyses assume constant heat input to the heating element (1 MW) to simulate steady state performance of a reactor while managing other transients in the integrated energy system. However, the heater operation is more complicated than the pump due to feedback between the resistive heating element and the electrical input that results from changes in material resistivity with temperature. Thus, feedback control based on temperature that changes the current and voltage outputs of the power supply is necessary. The specifics of the algorithm are dependent on the time constants associated with the heater material, cross-section geometry, and the characteristics of the power supply.

4.2.5 Velocity and Time Constants of the Primary Loop

Determination of the velocity of the secondary legs as a function of power output allows one to determine the time it takes for a heat/fluid transient to travel from the smart-valve to the heat-exchanger. This provides a rough time frame for the fan/VSD response.

The percent of mass flow that is sent to the power leg as a function of power output is given below:

$$\dot{m}_{\%,power} = \frac{P_{out} + 3942500}{4441000}$$

If we multiply this by the total mass flow rate, 16.7 kg/s, we get the mass flow to the power loop leg as a function of output. We then replace $\dot{m}_{power}$ with the equation for mass flow rate in terms of velocity, density, and cross-sectional area to obtain a relation for velocity as a function of power output.

$$\dot{m}_{power} = \dot{m}_{total}\dot{m}_{\%,power} = \rho A u_{power}$$

Density and cross section are constant, since the temperature is constant from the smart valve to the heat exchanger, and the area is static ($D = 0.061\ m$, as determined in Section 2.2.3). We can find density using the empirical equation for the working fluid (Dowtherm is assumed for the scaled facility) temperature-dependent density, and the area using the equation of the area of a circle (which is the geometry of the cross section):

$$\rho(T) = -0.898T + 1090 \rightarrow -0.898(186) + 1090 = 922.972\frac{kg}{m^3}$$
$$A = \frac{\pi D^2}{4} = \frac{\pi}{4}(0.061^2) = 2.9225 * 10^{-3}\ m^2$$

We can put these values into the equation for velocity and obtain the final relation:

$$u_{power} = \frac{\dot{m}_{total}\dot{m}_{\%,power}}{\rho A} = \frac{16.7}{(922.972)(2.9225 * 10^{-3})}\frac{P_{out} + 3942500}{4441000}$$

$$u_{power}(P_{out}) = \frac{P_{out} + 3942500}{717303}$$

We can also obtain the velocity of the HTSE leg by replacing $\dot{m}_{\%,power}$ with $(1 - \dot{m}_{\%,power})$:

$$u_{HTSE} = \frac{\dot{m}_{total}(1 - \dot{m}_{\%,power})}{\rho A} = \frac{16.7}{(922.972)(2.9225 * 10^{-3})}\frac{-P_{out} + 498500}{4441000}$$

$$u_{HTSE}(P_{out}) = \frac{-P_{out} + 498500}{717303}$$

Figure 18 shows a graph of the velocities as a function of the net power output of the scaled facility.

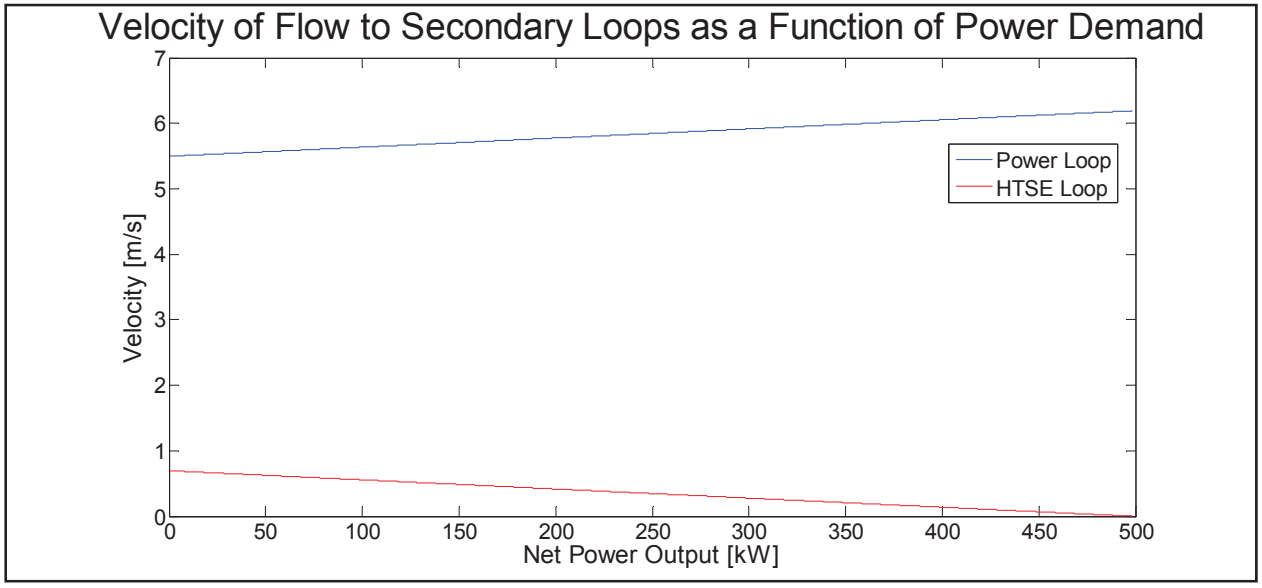

Figure 18. Graph of the velocities of the scaled facility's secondary legs of the primary loop, as a function of the simulated net power output.

The time required for the fluid to travel from the smart valve to the top of the two different heat exchangers is then determined by dividing the horizontal length by the velocity.

$$t_{power} = \frac{l}{u_{power}} = \frac{2.4375}{\frac{P_{out} + 3942500}{717303}} = \frac{1748426}{P_{out} + 3942500}$$

$$t_{HTSE} = \frac{l}{u_{HTSE}} = \frac{2.4375}{\frac{-P_{out} + 498500}{717303}} = \frac{1748426}{-P_{out} + 498500}$$

This result provides a *very* rough estimate of the relative time differences between each leg of the loop. These relations should be taken only as an initial estimate due to the immensely complex nature of fluid transients, especially given the rapid actuation of the valve during system operation. Detailed process flow analysis is required to support the actual loop design prior to sizing hardware and setting system flow rates.

5. Summary and Conclusions

This report lays out a preliminary scaling analysis for a 300 $MWth$ FHR-HTSE system's primary phenomena to be replicated in a non-nuclear 1 $MWth$ system. Dowtherm A was found to be an appropriate simulant fluid for the replication of the primary loop's Prandtl number. A primary leg pipe diameter of $0.061\ m$, and a primary leg mass flow rate of $16.7\ \frac{kg}{s}$, was found to be sufficient to match the Reynolds number of the prototype system, and thus duplicate the flow regime and friction factor in the scaled facility.

This analysis lays the groundwork for a facility that can replicate key thermophysical and fluid-dynamic phenomena of a prototype hybrid FHR, without having to deal with the costly and complicated nature of developing a full-scale nuclear energy system. In addition, this analysis leaves room for additional prototype components (such as the secondary process loops) to be scaled and added on to the facility. There is also room for the processes themselves (such as the HTSE) to be scaled and attached.

A key benefit to system analysis via a scaled test facility is the ability to easily investigate the effects of valve actuation on pressure surges and to quantify the resulting stress on the system components. The facility can be used to validate models run in parallel via computational fluid dynamic (CFD) software. This is an important point of analysis, as traditional nuclear designs do not have rapid actuation of mass flow rate and fluid velocity in such a central component of the system. It constitutes an unknown, both for steady-state operation and for accident-driven transients.

Another key benefit that comes with this scaled facility is the ability to test out feedback control algorithms, and their robustness in the face of hardware and software malfunctions. The facility can consistently be upgraded as analysis of the time constants and response times of various subcomponents is analyzed and incorporated via digital link-up or hardware add-ons. The facility can also be used to investigate the effects and stresses on components when the controls strategy sends fluid and heat in the wrong directions.

Preliminary scaling analysis focused on steady-state analysis and did not explicitly scale for transient phenomena. It will be necessary to go perform a more detailed analysis of scaled parameters for specific dimensionless numbers (such as the Strouhal number), although matching the Reynolds number should be sufficient to capture most of the transient characteristics. In addition, the materials properties of the various subsystems (such as the pipes) were not analyzed. This is an important area that should be analyzed prior to the implementation of the facility, as proper matching properties, such as pipe roughness, will have an effect on thermophysical and fluid-dynamic properties of the system as a whole. The materials properties will also have an effect on the pressure surges and shockwaves from rapid valve actuation, and the resultant stresses.

6. REFERENCES

Avigni, P. and B. Petrovic, "Fuel element and full core thermal-hydraulics analysis of the AHTR for the evaluation of the LOFC transient," *Annals of Nuclear Energy*, 2013 (In Press).

Bardet, Philippe M., Per F. Peterson, "Options for Scaled Experiments for High Temperature Liquid Salt and Helium Fluid Mechanics and Heat Transfer," *Nuclear Technology*, Vol. 163, September 2008.

Bragg-Sitton, S. M., R. Boardman, M. McKellar, H. Garcia, R. Wood, P. Sabharwall, and C. Rabiti, "Value Proposition for Load-Following Small Modular Reactor Hybrid Energy Systems," Idaho National Laboratory, INL/EXT-13-29298, May 2013.

Cammi, Antonio, et al., "A multi-physics modeling approach to the dynamics of Molten Salt Reactors. *Annals of Nuclear Energy*," Vol. 38, 2011, pp. 1356–1372.

Garcia, Humberto E., Amit. Mohanty, Wen-Chiao Lin, and Robert S. Cherry, "Dynamic analysis of hybrid energy systems under flexible operation and variable renewable generation – Part I: Dynamic performance analysis," *Energy*, 2013.

Garcia, Humberto E., Amit. Mohanty, Wen-Chiao Lin, and Robert S. Cherry, "Dynamic analysis of hybrid energy systems under flexible operation and variable renewable generation – Part II: Dynamic cost analysis," *Energy*, 2013.

Greene, Sherrell R., et al., "Pre-conceptual Design of a Fluoride-Salt-Cooled Small Modular Advanced High-Temperature Reactor (smAHTR)," Oak Ridge National Laboratory, ORNL/TM-2010/199, December 2010.

Incropera, Frank P. and David P. Dewitt, *Fundamentals of Heat and Mass Transfer*, 7th Edition, John Wiley and Sons, Hoboken, New Jersey, 2011.

Jianjun, Zhou, et al., "The influence of lower plenum and distribution plates to thermal hydraulics characteristics of MSRs," *Nuclear Engineering and Design*, Vol. 256, 2013, pp. 235–248.

Reyes, Jose N. Jr. and Lawrence Hochreiter, Scaling analysis for the OSU AP600 Test Facility (APEX). *Nuclear Engineering and Design*, Vol. 186, No. 1–2, 1998, pp. 53–109.

Sohal, Manohar S., Matthias A. Ebner, Piyush Sabharwall, and Phil Sharpe, "Engineering Database of Liquid Salt Thermophysical and Thermochemical Properties," Idaho National Laboratory. INL/EXT-10-18297, March 2010.

Stewart, James, *Multivariable Calculus: Early Transcendentals*, 6th Edition, Cengage Learning, 2007.

The Dow Chemical Company, "Dowtherm A Heat Transfer Fluid Product Technical Data," 1997.

Wood, R.A. and M. G. McKellar, "Hydrogen Production via FHR-Integrated High-Temperature Steam Electrolysis," Idaho National Laboratory, TEV-1776, March 2013.

Xiao, Yao, et al., "Numerical analysis for a molten salt reactor in the presence of localized perturbations," *Progress in Nuclear Energy*, Vol. 60, 2012, pp. 61–72.

Zuber, Novak, "Scaling: From Quanta to Nuclear Reactors," *Nuclear Engineering and Design*. Vol. 240, No. 8, 2010, pp. 1986–1996.

Appendix A

ASPEN Diagrams and Results Tables

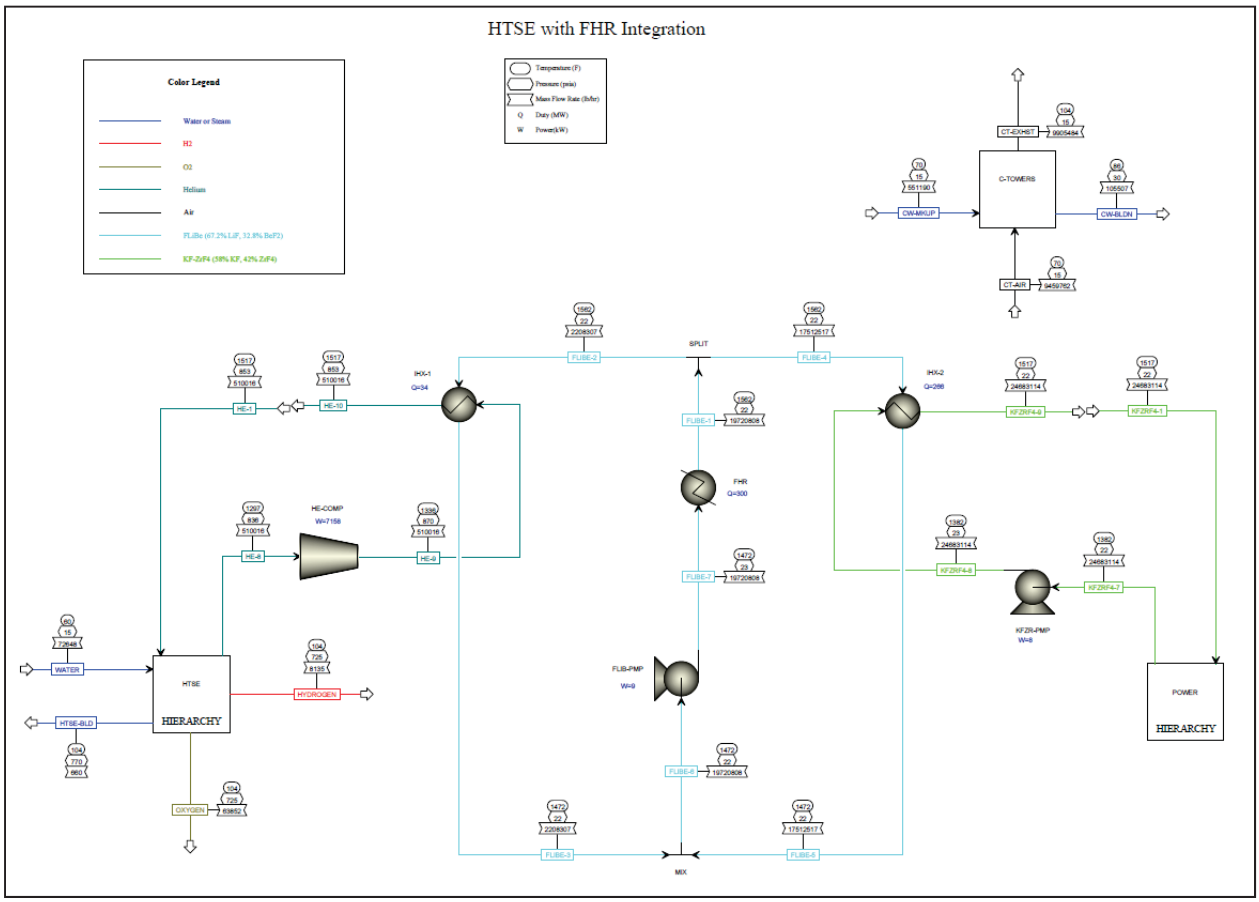

Figure A-1. ASPEN flowsheet of a 0 MWe power output system.

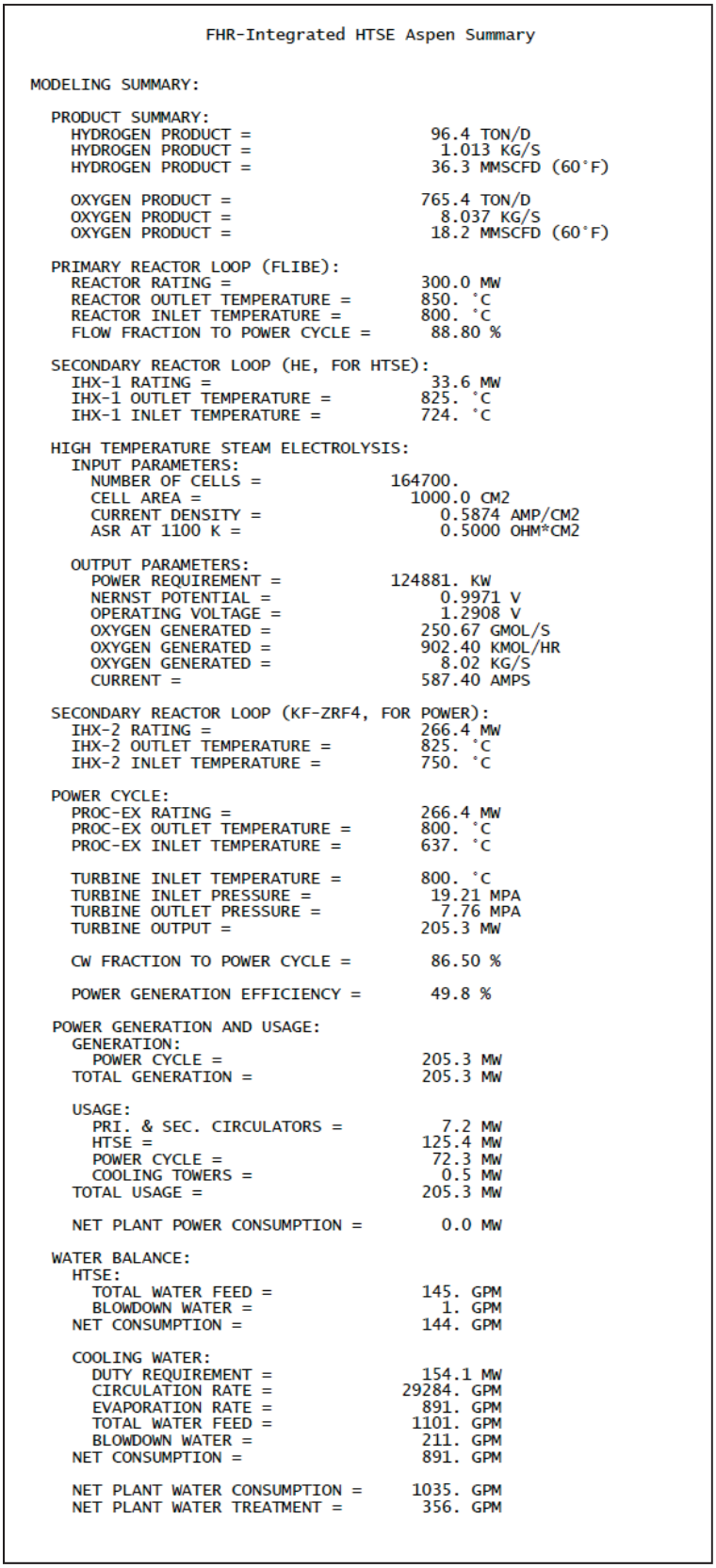

```
                FHR-Integrated HTSE Aspen Summary

MODELING SUMMARY:

  PRODUCT SUMMARY:
    HYDROGEN PRODUCT =                  96.4 TON/D
    HYDROGEN PRODUCT =                   1.013 KG/S
    HYDROGEN PRODUCT =                  36.3 MMSCFD (60°F)

    OXYGEN PRODUCT =                   765.4 TON/D
    OXYGEN PRODUCT =                     8.037 KG/S
    OXYGEN PRODUCT =                    18.2 MMSCFD (60°F)

  PRIMARY REACTOR LOOP (FLIBE):
    REACTOR RATING =                   300.0 MW
    REACTOR OUTLET TEMPERATURE =       850. °C
    REACTOR INLET TEMPERATURE =        800. °C
    FLOW FRACTION TO POWER CYCLE =      88.80 %

  SECONDARY REACTOR LOOP (HE, FOR HTSE):
    IHX-1 RATING =                      33.6 MW
    IHX-1 OUTLET TEMPERATURE =         825. °C
    IHX-1 INLET TEMPERATURE =          724. °C

  HIGH TEMPERATURE STEAM ELECTROLYSIS:
    INPUT PARAMETERS:
      NUMBER OF CELLS =             164700.
      CELL AREA =                    1000.0 CM2
      CURRENT DENSITY =                 0.5874 AMP/CM2
      ASR AT 1100 K =                   0.5000 OHM*CM2

    OUTPUT PARAMETERS:
      POWER REQUIREMENT =           124881. KW
      NERNST POTENTIAL =                0.9971 V
      OPERATING VOLTAGE =               1.2908 V
      OXYGEN GENERATED =              250.67 GMOL/S
      OXYGEN GENERATED =              902.40 KMOL/HR
      OXYGEN GENERATED =                8.02 KG/S
      CURRENT =                       587.40 AMPS

  SECONDARY REACTOR LOOP (KF-ZRF4, FOR POWER):
    IHX-2 RATING =                     266.4 MW
    IHX-2 OUTLET TEMPERATURE =         825. °C
    IHX-2 INLET TEMPERATURE =          750. °C

  POWER CYCLE:
    PROC-EX RATING =                   266.4 MW
    PROC-EX OUTLET TEMPERATURE =       800. °C
    PROC-EX INLET TEMPERATURE =        637. °C

    TURBINE INLET TEMPERATURE =        800. °C
    TURBINE INLET PRESSURE =            19.21 MPA
    TURBINE OUTLET PRESSURE =            7.76 MPA
    TURBINE OUTPUT =                   205.3 MW

    CW FRACTION TO POWER CYCLE =        86.50 %

    POWER GENERATION EFFICIENCY =       49.8 %

  POWER GENERATION AND USAGE:
    GENERATION:
      POWER CYCLE =                    205.3 MW
    TOTAL GENERATION =                 205.3 MW

    USAGE:
      PRI. & SEC. CIRCULATORS =          7.2 MW
      HTSE =                           125.4 MW
      POWER CYCLE =                     72.3 MW
      COOLING TOWERS =                   0.5 MW
    TOTAL USAGE =                      205.3 MW

    NET PLANT POWER CONSUMPTION =        0.0 MW

  WATER BALANCE:
    HTSE:
      TOTAL WATER FEED =               145. GPM
      BLOWDOWN WATER =                   1. GPM
    NET CONSUMPTION =                  144. GPM

    COOLING WATER:
      DUTY REQUIREMENT =               154.1 MW
      CIRCULATION RATE =             29284. GPM
      EVAPORATION RATE =               891. GPM
      TOTAL WATER FEED =              1101. GPM
      BLOWDOWN WATER =                 211. GPM
    NET CONSUMPTION =                  891. GPM

    NET PLANT WATER CONSUMPTION =     1035. GPM
    NET PLANT WATER TREATMENT =        356. GPM
```

Figure A-2. ASPEN summary of a 0 MWe power output system.

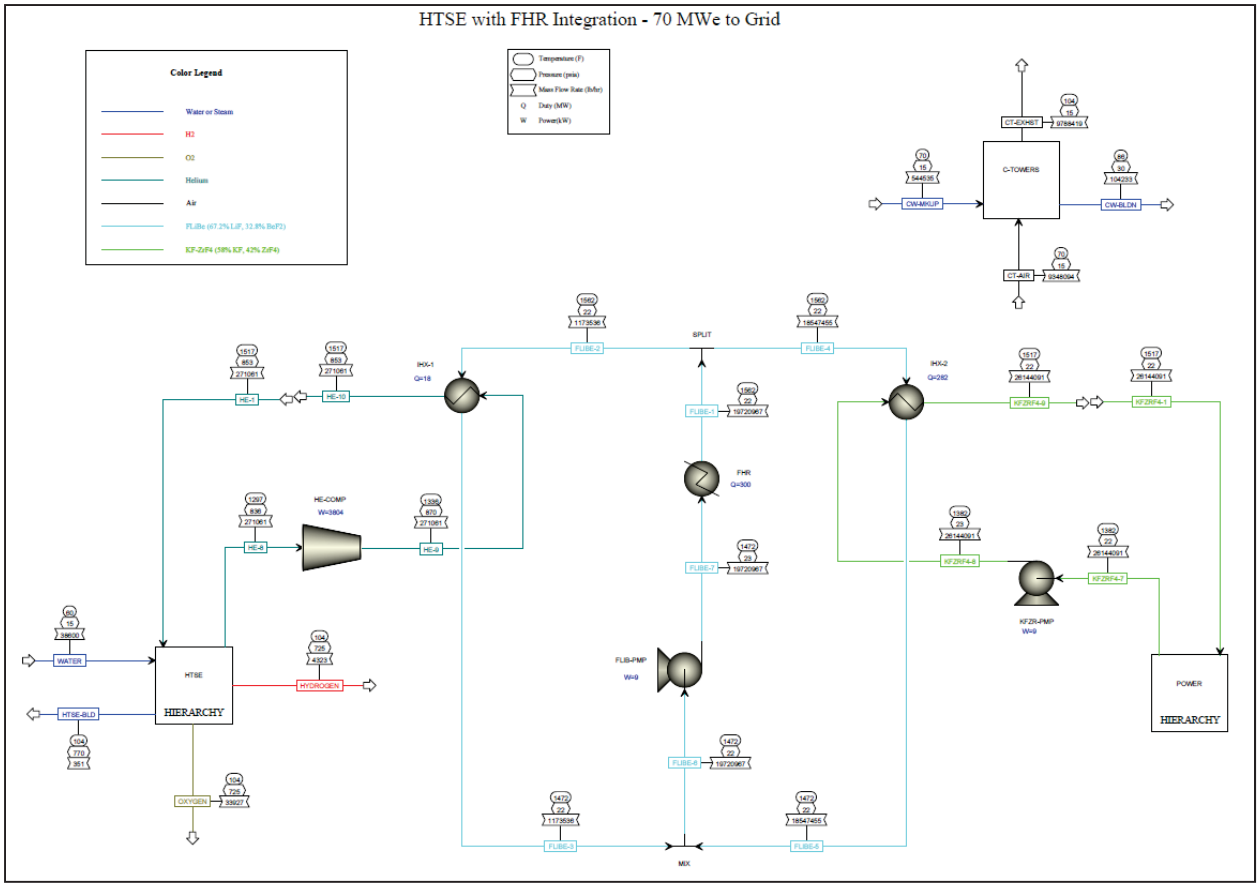

Figure A-3. ASPEN flowsheet of a 70 MWe power output system.

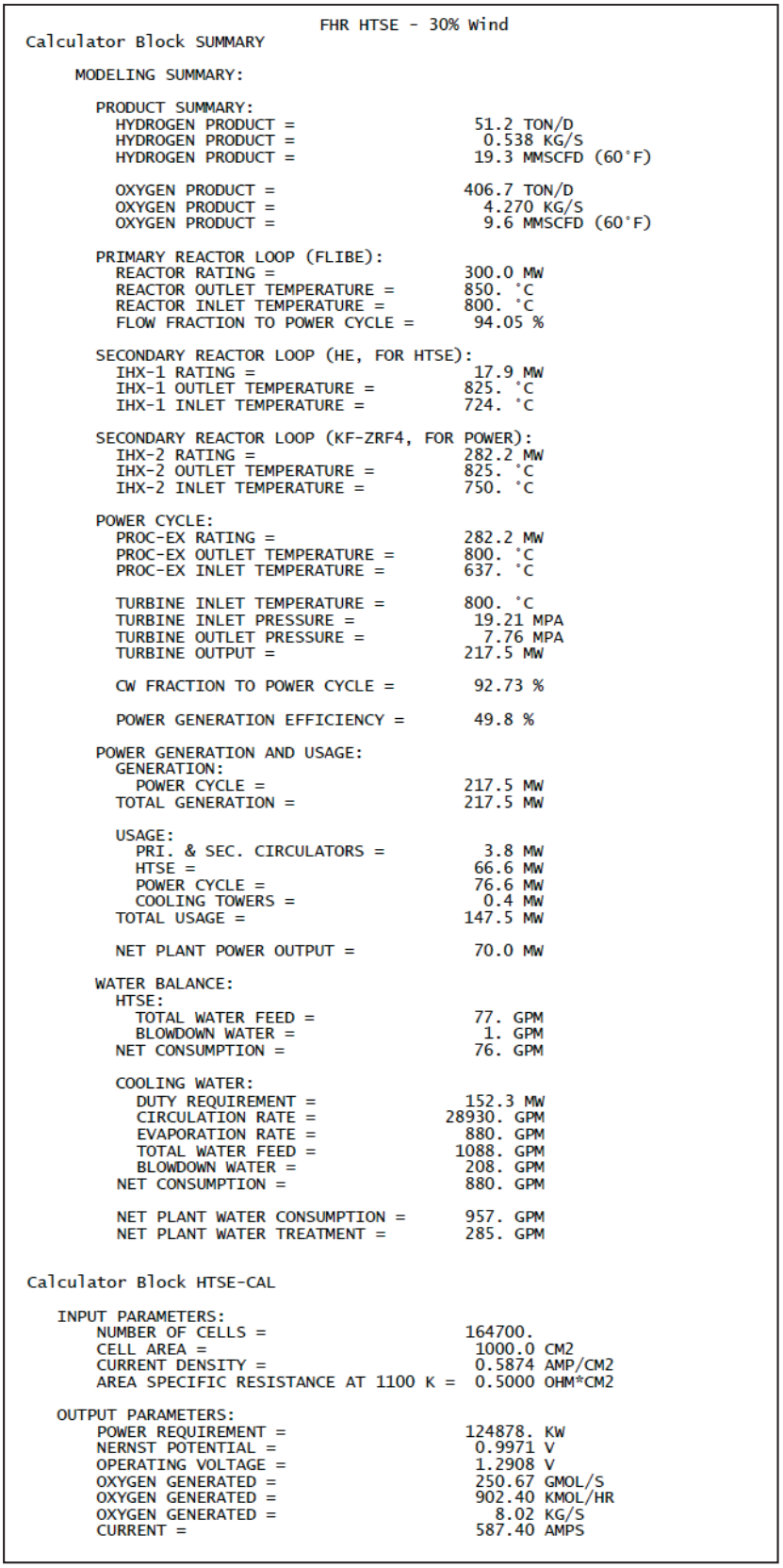

```
                                FHR HTSE - 30% Wind
Calculator Block SUMMARY

     MODELING SUMMARY:

       PRODUCT SUMMARY:
         HYDROGEN PRODUCT =                    51.2 TON/D
         HYDROGEN PRODUCT =                     0.538 KG/S
         HYDROGEN PRODUCT =                    19.3 MMSCFD (60°F)

         OXYGEN PRODUCT =                     406.7 TON/D
         OXYGEN PRODUCT =                       4.270 KG/S
         OXYGEN PRODUCT =                       9.6 MMSCFD (60°F)

       PRIMARY REACTOR LOOP (FLIBE):
         REACTOR RATING =                     300.0 MW
         REACTOR OUTLET TEMPERATURE =         850. °C
         REACTOR INLET TEMPERATURE =          800. °C
         FLOW FRACTION TO POWER CYCLE =        94.05 %

       SECONDARY REACTOR LOOP (HE, FOR HTSE):
         IHX-1 RATING =                        17.9 MW
         IHX-1 OUTLET TEMPERATURE =           825. °C
         IHX-1 INLET TEMPERATURE =            724. °C

       SECONDARY REACTOR LOOP (KF-ZRF4, FOR POWER):
         IHX-2 RATING =                       282.2 MW
         IHX-2 OUTLET TEMPERATURE =           825. °C
         IHX-2 INLET TEMPERATURE =            750. °C

       POWER CYCLE:
         PROC-EX RATING =                     282.2 MW
         PROC-EX OUTLET TEMPERATURE =         800. °C
         PROC-EX INLET TEMPERATURE =          637. °C

         TURBINE INLET TEMPERATURE =          800. °C
         TURBINE INLET PRESSURE =              19.21 MPA
         TURBINE OUTLET PRESSURE =              7.76 MPA
         TURBINE OUTPUT =                     217.5 MW

         CW FRACTION TO POWER CYCLE =          92.73 %

         POWER GENERATION EFFICIENCY =         49.8 %

       POWER GENERATION AND USAGE:
         GENERATION:
           POWER CYCLE =                      217.5 MW
         TOTAL GENERATION =                   217.5 MW

         USAGE:
           PRI. & SEC. CIRCULATORS =            3.8 MW
           HTSE =                              66.6 MW
           POWER CYCLE =                       76.6 MW
           COOLING TOWERS =                     0.4 MW
         TOTAL USAGE =                        147.5 MW

         NET PLANT POWER OUTPUT =              70.0 MW

       WATER BALANCE:
         HTSE:
           TOTAL WATER FEED =                  77. GPM
           BLOWDOWN WATER =                     1. GPM
         NET CONSUMPTION =                     76. GPM

         COOLING WATER:
           DUTY REQUIREMENT =                152.3 MW
           CIRCULATION RATE =              28930. GPM
           EVAPORATION RATE =                880. GPM
           TOTAL WATER FEED =               1088. GPM
           BLOWDOWN WATER =                  208. GPM
         NET CONSUMPTION =                   880. GPM

         NET PLANT WATER CONSUMPTION =       957. GPM
         NET PLANT WATER TREATMENT =         285. GPM


Calculator Block HTSE-CAL

    INPUT PARAMETERS:
        NUMBER OF CELLS =                    164700.
        CELL AREA =                           1000.0 CM2
        CURRENT DENSITY =                     0.5874 AMP/CM2
        AREA SPECIFIC RESISTANCE AT 1100 K =  0.5000 OHM*CM2

    OUTPUT PARAMETERS:
        POWER REQUIREMENT =                  124878. KW
        NERNST POTENTIAL =                    0.9971 V
        OPERATING VOLTAGE =                   1.2908 V
        OXYGEN GENERATED =                    250.67 GMOL/S
        OXYGEN GENERATED =                    902.40 KMOL/HR
        OXYGEN GENERATED =                      8.02 KG/S
        CURRENT =                             587.40 AMPS
```

Figure A-4. ASPEN summary of a 70 MWe power output system

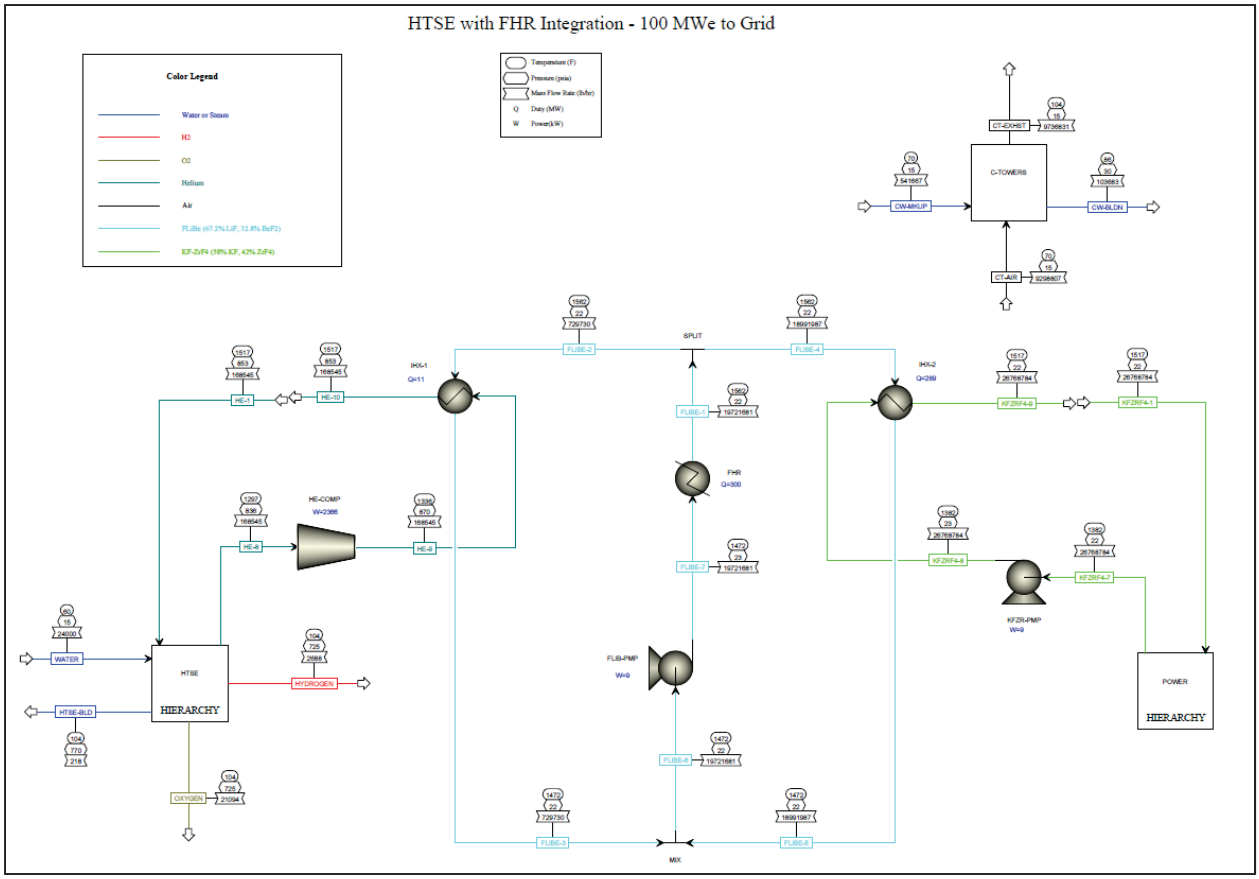

Figure A-5. ASPEN flowsheet of a 100 MWe power output system.

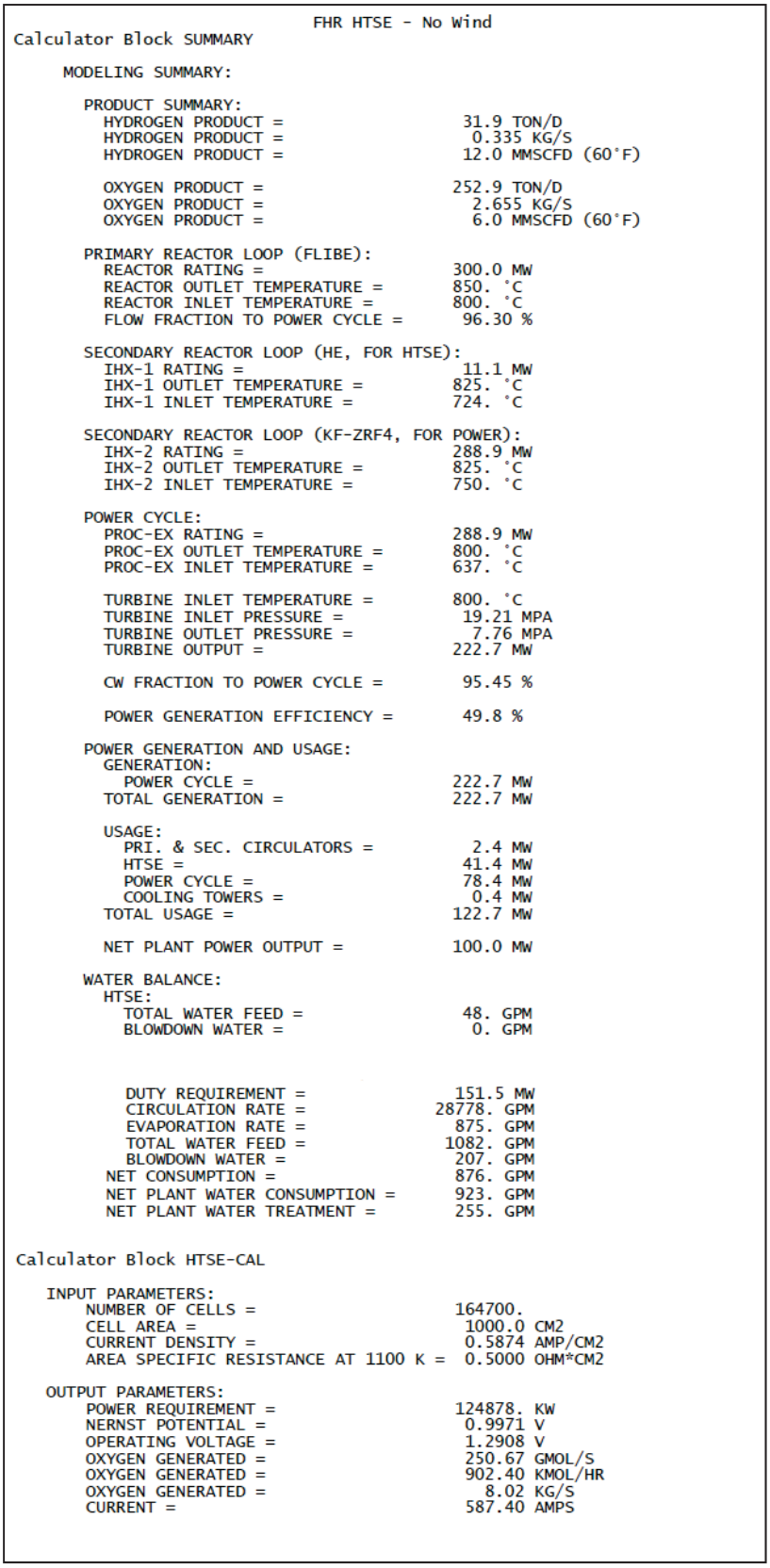

```
                                FHR HTSE - No Wind
Calculator Block SUMMARY

     MODELING SUMMARY:

       PRODUCT SUMMARY:
         HYDROGEN PRODUCT =                  31.9 TON/D
         HYDROGEN PRODUCT =                   0.335 KG/S
         HYDROGEN PRODUCT =                  12.0 MMSCFD (60°F)

         OXYGEN PRODUCT =                   252.9 TON/D
         OXYGEN PRODUCT =                     2.655 KG/S
         OXYGEN PRODUCT =                     6.0 MMSCFD (60°F)

       PRIMARY REACTOR LOOP (FLIBE):
         REACTOR RATING =                   300.0 MW
         REACTOR OUTLET TEMPERATURE =       850. °C
         REACTOR INLET TEMPERATURE =        800. °C
         FLOW FRACTION TO POWER CYCLE =      96.30 %

       SECONDARY REACTOR LOOP (HE, FOR HTSE):
         IHX-1 RATING =                      11.1 MW
         IHX-1 OUTLET TEMPERATURE =         825. °C
         IHX-1 INLET TEMPERATURE =          724. °C

       SECONDARY REACTOR LOOP (KF-ZRF4, FOR POWER):
         IHX-2 RATING =                     288.9 MW
         IHX-2 OUTLET TEMPERATURE =         825. °C
         IHX-2 INLET TEMPERATURE =          750. °C

       POWER CYCLE:
         PROC-EX RATING =                   288.9 MW
         PROC-EX OUTLET TEMPERATURE =       800. °C
         PROC-EX INLET TEMPERATURE =        637. °C

         TURBINE INLET TEMPERATURE =        800. °C
         TURBINE INLET PRESSURE =            19.21 MPA
         TURBINE OUTLET PRESSURE =            7.76 MPA
         TURBINE OUTPUT =                   222.7 MW

         CW FRACTION TO POWER CYCLE =        95.45 %

         POWER GENERATION EFFICIENCY =       49.8 %

       POWER GENERATION AND USAGE:
         GENERATION:
           POWER CYCLE =                    222.7 MW
         TOTAL GENERATION =                 222.7 MW

         USAGE:
           PRI. & SEC. CIRCULATORS =          2.4 MW
           HTSE =                            41.4 MW
           POWER CYCLE =                     78.4 MW
           COOLING TOWERS =                   0.4 MW
         TOTAL USAGE =                      122.7 MW

         NET PLANT POWER OUTPUT =           100.0 MW

       WATER BALANCE:
         HTSE:
           TOTAL WATER FEED =                48. GPM
           BLOWDOWN WATER =                   0. GPM


           DUTY REQUIREMENT =              151.5 MW
           CIRCULATION RATE =            28778. GPM
           EVAPORATION RATE =              875. GPM
           TOTAL WATER FEED =             1082. GPM
           BLOWDOWN WATER =                207. GPM
         NET CONSUMPTION =                 876. GPM
         NET PLANT WATER CONSUMPTION =     923. GPM
         NET PLANT WATER TREATMENT =       255. GPM

Calculator Block HTSE-CAL

   INPUT PARAMETERS:
       NUMBER OF CELLS =                  164700.
       CELL AREA =                         1000.0 CM2
       CURRENT DENSITY =                   0.5874 AMP/CM2
       AREA SPECIFIC RESISTANCE AT 1100 K =  0.5000 OHM*CM2

   OUTPUT PARAMETERS:
       POWER REQUIREMENT =                124878. KW
       NERNST POTENTIAL =                  0.9971 V
       OPERATING VOLTAGE =                 1.2908 V
       OXYGEN GENERATED =                  250.67 GMOL/S
       OXYGEN GENERATED =                  902.40 KMOL/HR
       OXYGEN GENERATED =                    8.02 KG/S
       CURRENT =                           587.40 AMPS
```

Figure A-6. ASPEN summary of a 100 MWe power output system.